University of Pretoria etd – Meyer, W E (2007)

8

DLTS observation of the transformation of bistable defects

8.1 Introduction

Most defects in semiconductors have, for a given charge state, a single fixed atomic configuration. Consequently, the deep levels due to these defects remain detectable under a wide range of experimental conditions, and their properties do not depend on the history of the sample. However, there are deep levels that are easily removed and re-introduced by relatively small changes in experimental conditions. An example of such conditions that may remove and re-introduce these defects is annealing under forward or reverse bias (i.e. in the presence or absence of electrons). This behaviour of defects suggests that these defects have more than one structural configuration in at least one charge state. Defects having two structural configurations are called configurationally bistable, while those with more than two structural configurations are referred to as being multistable.

From a technological point of view, these defects are important since their complex behaviour may lead to erratic behaviour of devices manufactured on material containing the defect, as illustrated by the Thermal Donors in Silicon (Chantre, 1989). From a scientific point of view, these defects allow the measurement of certain parameters (e.g. transformation activation energy) that can shed more light on the accuracy of theoretical models. In the long term, defect metastability may become interesting as an information storage technology.

The standard method used to detect defect bistability by means of DLTS, is to compare two DLTS temperature scanned spectra, recorded upwards in temperature, after cooling the sample under zero and reverse-bias conditions respectively. Any differences between these two spectra are probably due to defects changing their configurations due to the applied bias, before the sample was cooled down. See, for instance, Levinson (1985). However, during the recording of a spectrum, an LIA DLTS system continuously exposes the sample to filling pulses. Since these filling pulses also change the charge state of the defect, they may also transform the defect to another configuration. LIA DLTS is therefore not the ideal technique to characterise metastable defects.

However, in a digital DLTS system, it is possible to make "one shot" measurements, where only a single filling pulse is applied, therefore almost eliminating the danger of unintentionally transforming the defect. In this study, we used the digital DLTS system to characterise the electronic and metastable properties of an α-particle induced defect in epitaxially-grown boron-doped p-type silicon. A copy of two papers that followed from the research is included at the end of the chapter.

Originally, Mamor discovered and characterised the defect by means of an LIA DLTS system. However, due to the limitations of the LIA DLTS system, data could only be recorded over a limited range, and significant scatter and systematic errors were evident. The present author repeated the measurements and calculations with the digital DLTS system described in this work, provided the results in the publication, and wrote a significant portion of the paper (amongst others, all of the experimental section involving isothermal DLTS and the characterisation of the metastable properties of the defect, as well as most of the discussion of the metastable properties of the defect.)

8.1.1 Configurationally bistable defects

Configurationally bistable defects are defects in which at least one charge state has two possible atomic configurations that achieve a local minimum in the total energy of the defect. (The total energy of the defect is the sum of the electronic and the elastic energy.) The best way to describe configurational defect metastability is by making use of a configuration coordinate (CC) diagram. This diagram is a schematic graph of the total energy of the defect, drawn for every relevant charge state of the defect as a function of the configuration coordinate. The configuration coordinate represents the degree to which the atoms comprising the defect are in either of the two configurations.

For most monatomic defects (e.g. a substitutional dopant in Si), the position of the minimum energy on the CC-axis does not depend on the charge state of the defect. However, for some defects (e.g. the DX centre in AlGaAs) a change in charge state causes a significant lattice relaxation. The CC diagrams corresponding to a "normal" and a large lattice relaxation defect are shown in Figure 8.1(a) and (b) respectively.

It is clear from their CC diagrams that the defects (a) and (b) discussed in the previous paragraph both have a unique stable atomic arrangement for a given charge state. This does not have to be the case. Consider the CC diagrams shown in Figure 8.1(c) and (d). These defects have two different stable structural configurations in at least one charge state and are referred to as being *bistable*. In one charge state, the configuration with the higher energy is called the metastable configuration, while the other is

called the stable configuration. The two configurations are separated by a barrier. If the defect is in some way placed in the metastable configuration, it will in time decay to the stable configuration. This transformation is generally thermally activated.

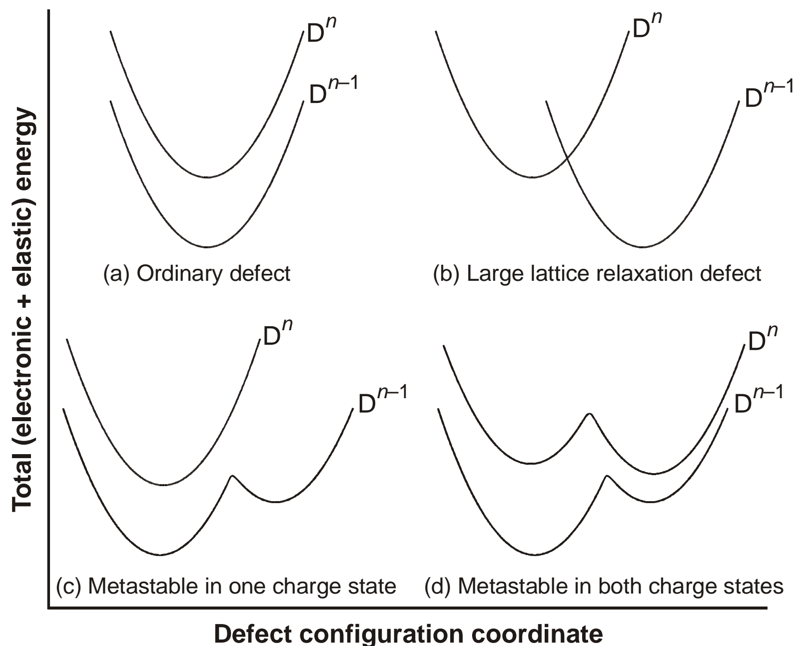

Figure 8.1 *Configuration coordinate diagrams for a number of different types of defects. (After Chantre, 1989).*

Some defects exhibiting metastable properties are the Thermal Donor in Si (Chantre, 1987), which seems to be bistable in only one charge state [as illustrated in Figure 8.1(c)], and Fe–Al and C–C pairs Greulich-Weber (1991) and Song (1988) in Si which seem to display bistability in all charge states [Figure 8.1(d)]. Multistable defects, having more than one metastable state, have also been observed in Si by Zhan (1993).

8.1.2 Charge state controlled metastability

In order for the phenomenon to be observable by means of DLTS, the stable configuration of a defect should change with charge state, and there should be a significant barrier for conversion between the charge states. Consider the CC shown in Figure 8.2. The defect has two possible structural configurations in both its neutral (0) and ionised states. However, in the neutral state, configuration A is stable, while in its ionised state, configuration B is energetically more favourable. In the following explanation it is assumed that the activation energy in both directions is such that at 300 K the transformation barriers $E_a(0)$ and $E_a(+)$ are easily surmounted, but at 100 K the defect is effectively "frozen" in its current state.

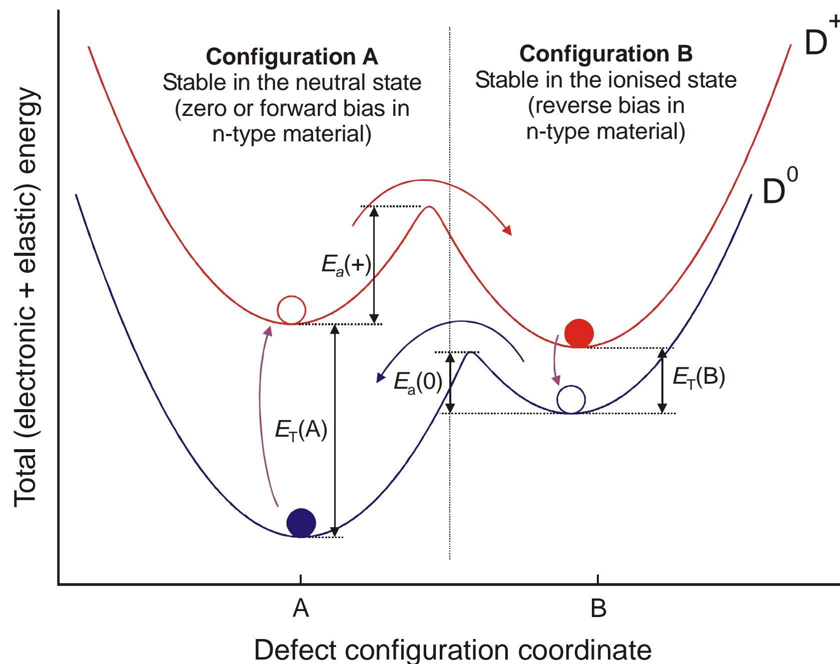

Figure 8.2 *Schematic diagram of a defect having two configurations, each configuration being stable in a different charge state. E.g. in the neutral state (lower curve) the defect is stable in configuration A, while in its ionised state, it is stable in configuration B (After Chantre, 1989).*

When the sample is at 300 K, the defect can be switched between configurations A and B by changing the charge state of the defect between its ionised and neutral states. In the area beneath a Schottky contact, this can be done by applying a suitable bias. For an n-type semiconductor, a forward bias would fill the defect level with an electron, leaving the defect in our example in its neutral state. Since configuration A is more stable in the neutral state, most of the defects will be in configuration A. Similarly a reverse bias would allow the defect level to emit an electron, thereby leaving the defect in its positively ionised state, which favours configuration B.

If the sample is cooled down to 100 K without changing the bias conditions, the stable configuration (either A or B, depending on the applied bias) will be frozen in. If, at this low temperature, the emission and capture rate of the defect is much higher than the transformation rate, the charge state of the defect can now be changed by changing applied bias, in principle without affecting the defect's configuration.

Once the defect has been transformed to the required configuration, it may be studied by means of DLTS. In the idealised case, one would expect to observe a DLTS peak associated with each of the configurations. However, in order to observe the DLTS peak, the associated defect has to remain stable while it is occupied by a carrier. There are a number of defects (including the one discussed by Mamor, 1998) where one of the transformation processes cannot be separated from carrier emission from the defect. In these cases, only one state can be observed by means of DLTS.

Although the most common technique to isolate and characterise charge-state controlled bistable defects is DLTS combined with bias-on/bias-off annealing cycles, other techniques to modulate the Fermi level (e.g. incident light or doping) are also used, see for instance Kaczor (1993)

8.1.3 Characterisation of metastable defects

In order to characterise a metastable defect completely, one would like to know the atomic structure in the various configurations as well as the physical mechanisms by means of which the defect transforms. As an intermediate step, the transformational properties of the defect can be summarised on a CC diagram. This implies determining the electronic energy levels in each configuration as well as the kinetics of the transformation.

Usually, the transformation occurs via first-order kinetics, with the transformation rate R thermally activated, according to

$$R = R_0 e^{-E_a / kT}$$

where E_a is the activation energy. The preexponential factor R_0 can be physically related to the attempt frequency of the process and can be used to deduce the physical mechanism leading to the temperature dependence. Some mechanisms identified so far are (Chantre, 1989):

i) elementary atomic jump ($R_0 \sim 10^{12}\ \mathrm{s}^{-1}$)
ii) free-carrier capture by multiphonon emission ($R_0 \sim 10^{7}\ \mathrm{s}^{-1}$)
iii) free-carrier emission ($R_0 \sim 10^{13}\ \mathrm{s}^{-1}$)

8.1.4 Example: The C–C pair in Si

The physical structure of most metastable defects has not yet been identified. However, a well-researched example is the C–C pair in Si, reported by Song (1988), which consists of an interstitial carbon atom paired with a substitutional carbon atom. This defect can exist in two configurations called A and B, which differ only by a simple bond switching transformation, as shown in Figure 8.3.

Configuration A is stable for both the positively charged $(C_iC_s)^+$ and negatively charged $(C_iC_s)^-$ states, but for the neutral $(C_iC_s)^0$ state, Configuration B is stable. In their paper, Song et al. give a detailed discussion of how the properties of this defect were determined using DLTS, electron paramagnetic resonance (EPR) and optical detection of magnetic resonance (ODMR) results.

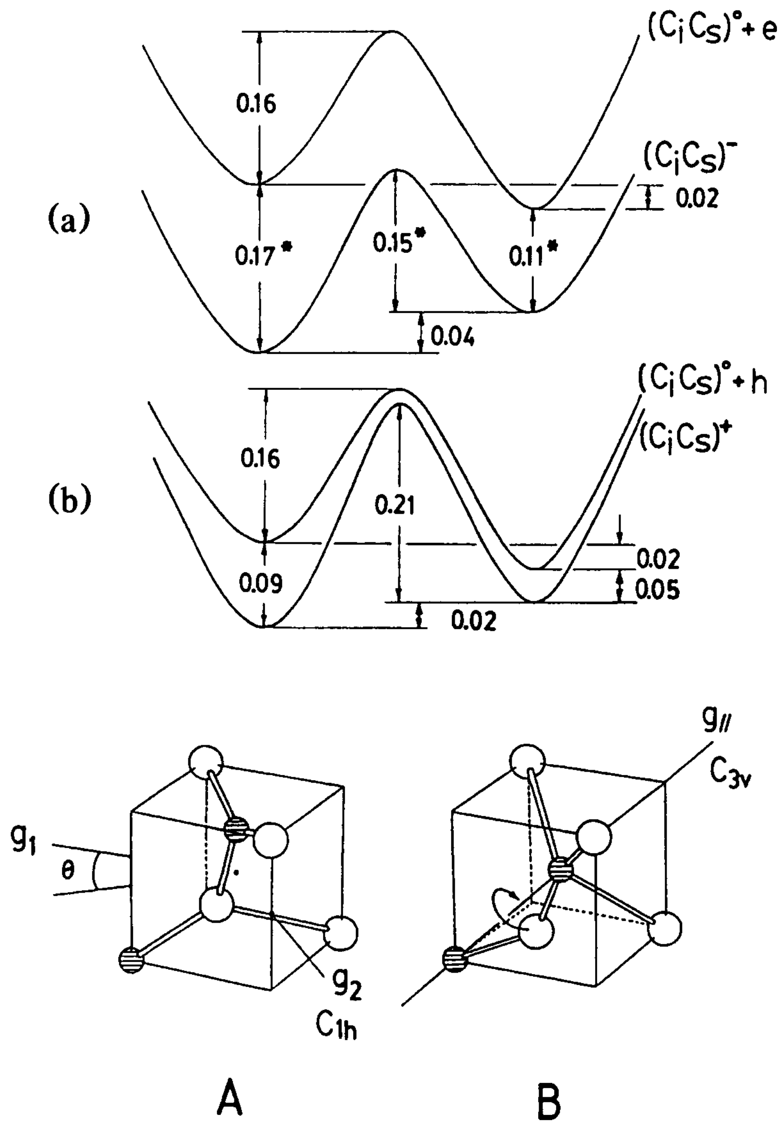

Figure 8.3 *C-C diagrams and sketches showing the metastable transformation of the C-C pair in Silicon. (Song, 1988)*

8.2 Experimental

8.2.1 Introduction

In this section, the results of an investigation into the metastable behaviour of an α-particle induced defect in epitaxially grown boron-doped p-type silicon are presented. The defect was originally detected and characterised by a conventional LIA-based DLTS system. During analysis of the data, it became clear that, due to the defect transforming during the repetitive filling pulse applied by the LIA-

based DLTS system, it was difficult to characterise the defect completely. The characterisation process was repeated, this time with the digital DLTS system, which yielded more reliable results, especially at higher temperatures where the defects would transform too fast for an LIA-based DLTS system to detect. Since single transients could be recorded and arbitrary long filling pulses could be applied, the digital system allowed for experimental conditions to be tailored to measure the transformation kinetics of the defect in a temperature range that was not accessible to the LIA-based system. These results from the digital system were used to augment the results obtained from the analogue system. See Figure 4 in Mamor (1998) and associated discussion.

8.2.2 Sample preparation

The sample was prepared according to the standard procedure mentioned in Chapter 5. After evaporation of the titanium Schottky contacts, the sample was irradiated through the contacts by 5.4 MeV α-particles from an americium 241 (Am-241) radionuclide to a fluence of 1×10^{12} cm^{-2}.

8.2.3 Determining the defects' DLTS signatures

The LIA DLTS spectrum of the sample is shown in Figure 8.4. Here it can be seen that defect Hα2 exhibits metastable properties – when the sample is cooled down under zero bias the Hα2 peak disappears (dotted line, State A), only to reappear when the sample is heated to 300 K and cooled down under reverse bias (solid line, State B). Because the Hα1 peak partially overlaps with the Hα2 peak, it is not possible to observe Hα2 in isolation without some processing. In order to isolate Hα2, the "zero-bias" scan (containing only Hα1) was subtracted from the "reverse-bias" scan (containing both Hα1 and Hα2, leaving a scan containing only Hα2, indicated by the dashed line in Figure 8.4.

The defects' DLTS signatures were determined in the usual way from Arrhenius plots in which $\ln(e/T^2)$ is plotted as a function of $1/T$ (see Section 2.2.1). The data for the Hα2 was obtained from the subtracted scans.

At higher temperatures, the Hα2 (state B) peak was quickly transformed by removal of the reverse bias. This also occurred during the relatively short DLTS filling pulse. It was found that, in the LIA-based DLTS system, where the sample was continuously exposed to the filling pulses, the cumulative effect of these filling pulses would soon remove the Hα2 completely. This process limited the maximum temperature at which the sample could be measured by an LIA-based system to approximately 220 K. On the other end of the scale, the lowest temperature at which the sample could be measured was limited to 200 K by the maximum period at which the LIA could still record a signal. Due to these two constraints, the temperature range over which data for an Arrhenius plot could be collected by the LIA-system was limited to a 20 K range between 200 and 220 K.

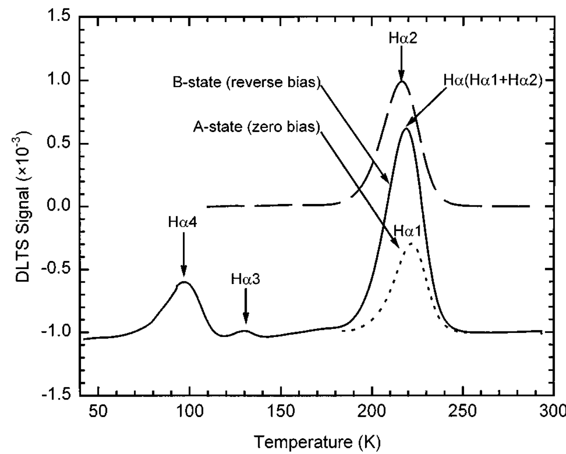

Figure 8.4 *LIA DLTS of the Hα2 peak measured after cool down under forward and reverse bias respectively, showing its metastable properties. (Mamor, 1998)*

Since the digital DLTS system only needed to record a single transient, only a single filling pulse was required, thereby minimising the transformation due to the DLTS filling pulse. Furthermore, the digital system could record much longer transients than the LIA-based system, so it was possible to measure at much lower temperatures as well. The results of these measurements are shown in Figure 8.5. For comparison, the values obtained from the LIA-based system are also shown. Although these points lie in the same vicinity as those obtained from the digital system, they show more scatter and, as discussed earlier, they cover a much narrower range.

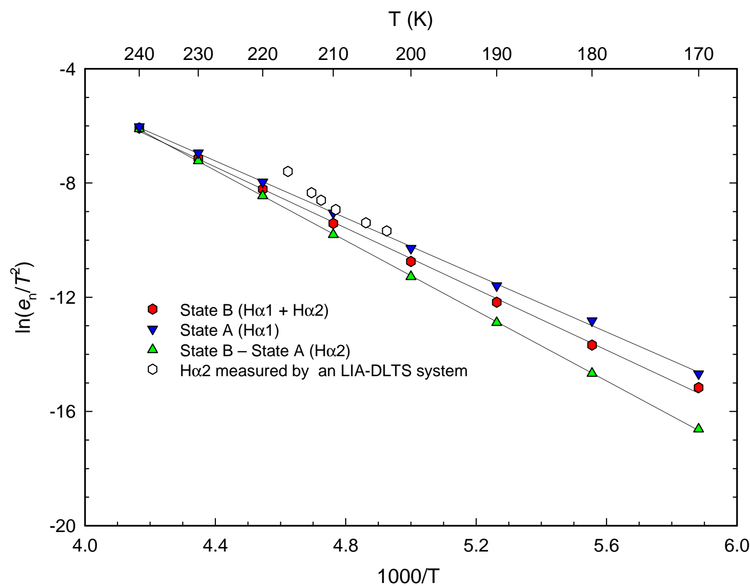

Figure 8.5 *Arrhenius plots of the Hα1, Hα2 and (Hα1 + Hα2) peaks as obtained by the digital DLTS system (filled symbols). The graph also shows the points determined by means of a conventional LIA-DLTS system (open circles).*

8.2.4 Determination of the transformation kinetics

In an LIA DLTS system, the standard procedure to measure the transformation rate of a metastable defect from state B to state A is to first transform the defect completely to state B. The peak height of state B is then measured by means of DLTS. Hereafter the sample is now repeatedly annealed for a specified period under conditions favouring state A, and the peak height due to the defects remaining in state B is measured after every annealing cycle. If the peak height is plotted as a function of total annealing time, one should obtain an exponential decay curve from which the decay constant can be determined.

By repeating this procedure at different temperatures, these decay constants can be used to determine the activation energy of the defect as described in Section 8.1.3.

Although the technique above seems quite straightforward, it relies on a number of assumptions:

1. Since it takes a finite time to heat the sample to the annealing temperature, the annealing time is never exact. This is particularly significant at higher temperatures when the transformation rate of the defect is high, and the time required to reach the annealing temperature is significant compared to the annealing time.

2. As described earlier, depending on the temperature at which the defect is measured, the defect may transform during the DLTS scan.

8.2.4.1 The transformation B → A

By means of the digital DLTS system, it was possible to measure the amplitude of the DLTS transient due to the defects at the annealing temperature. During this procedure, the sample was first annealed under reverse bias for a sufficient time to convert all the defects to state B. The transformation B → A was now allowed to occur by applying a single forward-bias transformation pulse to the defect. The pulse also filled the defect, and was therefore followed by a DLTS transient. This transient was not of interest, and was allowed to decay. Hereafter a second much shorter measuring pulse was applied and the resulting transient was recorded. By varying the length of the first pulse, and measuring the amplitude of the second transient, it was possible to determine the transformation rate of the defect.

It is interesting to note that the procedure described above leads to the rather counterintuitive result namely that, over the pulse length range of interest, longer filling pulses caused smaller DLTS transients.

8.2.4.2 The transformation A → B

By using the digital DLTS system, it was possible to observe the transformation of the defect more directly. It was observed from TSCAP measurements that the transformation A → B is associated with the emission of a hole. However, it was not clear whether the emission of the hole occurred as part of or directly after the transformation process. However, DLTS measurements show that hole emission from the B state occurred much faster than the transformation A → B; therefore, the emission of the hole (as

detected by DLTS) could be used as a reliable measure of the transformation. It was thus possible to observe this transformation directly by means of DLTS, as long as the DLTS filling pulse was long enough to convert a significant fraction of the defect to state A.

8.2.5 Discussion

The results of this research was published in the papers Mamor (1998) and Mamor (2000). The extended range allowed by the digital DLTS system is clearly shown in Figure 8.5, where the results obtained by the digital system are shown using solid symbols while the LIA-results are shown using open symbols. The results obtained by the digital system agreed well with those obtained by means of the analogue system. It is clear that the digital system extended the range and accuracy of the measurements significantly.

8.3 Publications

The results of this study on the Hα1 and Hα2 defects were published in the following publications. All digital DLTS measurements and associated calculations and discussion of the metastability were by the present author.

1. Mamor M, Auret FD, Goodman SA, Meyer WE and Myburg G 1998 Electronic and transformation properties of a metastable defect introduced in epitaxially grown boron-doped p-type Si by alpha particle irradiation *Appl. Phys. Lett.* **72** 3178

2. Mamor M, Willander M, Auret FD, Meyer WE and Sveinbjörnsson E 2000 Configurationally metastable defects in irradiated epitaxially grown boron-doped p-type Si *Phys. Rev. B* **63** 045201

University of Pretoria etd – Meyer, W E (2007)

APPLIED PHYSICS LETTERS VOLUME 72, NUMBER 24 15 JUNE 1998

Electronic and transformation properties of a metastable defect introduced in epitaxially grown boron-doped *p*-type Si by alpha particle irradiation

M. Mamor,[a] F. D. Auret, S. A. Goodman, W. E. Meyer, and G. Myburg
Physics Department, University of Pretoria, Pretoria 0002, South Africa

(Received 17 December 1997; accepted for publication 14 April 1998)

Titanium (Ti) Schottky barrier diodes on epitaxially grown boron-doped p-type Si films with a free carrier density of $6-8\times 10^{16}$ cm^{-3} were irradiated with alpha particles at room temperature using an americium-241 (Am-241) radio nuclide. We report the electronic and transformation characteristics of an α-particle irradiation-induced defect $H\alpha 2$ in epitaxially grown p-Si with metastable properties. The energy level and apparent capture cross section, as determined by deep-level transient spectroscopy, are $E_v+0.43$ eV and 1.4×10^{-15} cm^2, respectively. This defect can be removed and re-introduced using a conventional bias-on/off cooling technique. © *1998 American Institute of Physics.* [S0003-6951(98)03424-X]

Several investigations of the metastability of defects in as-grown Si as well as in as-grown GaAs and InP have been reported in the last few years by several workers.[1–4] The metastable configuration can normally be detected by deep-level transient spectroscopy (DLTS). Using the bias-on bias-off cooling technique and annealing cycles, these metastable defects are configurationally transformed to different energy states, which can usually be detected by DLTS. A significant number of metastable defects investigated in Si,[5] GaAs,[6] and InP,[4] were introduced by electron irradiation. In ultrafast quenched (laser irradiated) boron-doped Si a defect has been detected by capacitance spectroscopy (the C center after Chantre[7]) with metastable characteristics. This center was shown to exist in either of two configurations A or B, depending on its charge state. More recently, minority carrier injection combined with the bias-on bias-off cooling technique has led to the detection of a metastable defect in α-irradiated GaAs.[8] Hence, it is reasonable to expect that irradiation with other particle types would also introduce metastable defects in bulk grown Si as well as in epitaxially grown Si.

In this letter we demonstrate that, apart from a metastable electron irradiation induced defect in Si,[5] a prominent defect in α-irradiated epitaxially grown boron-doped Si is also metastable.

In this study, we used Schottky barrier diodes (SBDs) as the contact structure to the epitaxially grown Si. The Si samples studied were grown by chemical vapor deposition (CVD). Circular titanium contacts, 0.77 mm in diameter and 200 nm thick, were deposited by electron-beam evaporation onto p-Si at rate of 10 Å/s, through a metal contact mask. A metal shield was positioned to prevent stray electrons originating from filament from reaching the Si layers. The free carrier concentration (N_A-N_D) induced by boron doping of the epitaxial Si layers, as determined by capacitance–voltage ($C-V$) measurements, was $6-8\times 10^{16}$ cm^{-3}. An americium 241 (Am-241) radionuclide with an activity of 192 μCi cm^{-2} was used to irradiate the samples with 5.4 MeV α particles at a fluence rate of 7.1×10^6 cm^{-2} s^{-1}. As it is assumed that the measured capacitance transient varies exponentially with time, it is important that the densities of introduced deep levels are small compared to those of shallow levels. The trap density (N_T) should not be greater than 10% of the free carrier density (N_A-N_D) to ensure exponential transients.[9]

The α-particle induced defects in the Si epilayer were characterized by DLTS[10] using a lock-in amplifier (LIA) based system. The energy level (E_t) in the band gap and apparent capture cross section (σ_a) of defects were determined from Arrhenius plots of T^2/e vs $1/T$, where e is the emission rate at a temperature T.

The data for the Arrhenius plots were measured by means of an isothermal DLTS technique. The DLTS capacitance transient was measured by a Boonton 7200 capacitance meter and digitized by an HP 3458A multimeter. The digitized transient was analyzed with a "simulated lock-in amplifier" technique. This technique has the advantage that, depending on the signal quality, only a single transient is required to determine the emission rate of a defect at a given temperature. Furthermore, compared to an analogue lock-in amplifier, the digitally simulated lock-in amplifier allows for a wider range of emission rates to be observed, thus extending the temperature range over which the Arrhenius data could be measured. Unwanted transformation of the defect before the DLTS measurement was minimized by keeping the sample at the bias conditions under which it was annealed until the temperature for DLTS measurements was reached. The bias conditions for DLTS were applied only directly before the DLTS measurements were made. Since the isothermal DLTS technique described above requires only a single transient, the sample experienced only a single pulse that could transform the defect. In order to further minimize the risk of the defect being transformed by this single pulse, the rising edge of the DLTS filling pulse was shaped carefully to avoid overshoot, and the pulse was kept reasonably short (0.1 ms). By employing these techniques, it was possible to see both defect peaks at temperatures as high as 240 K. However, at 240 K the peak height of the subtracted spectrum was lower than in the other measurements,

[a]Electronic mail: mmamor@scientia.up.ac.za

 © 1998 American Institute of Physics

University of Pretoria etd – Meyer, W E (2007)

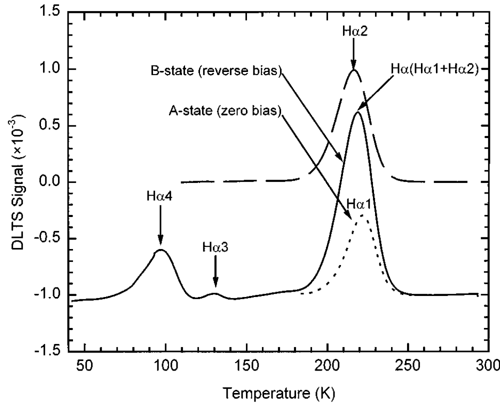

FIG. 1. DLTS spectra of p-type Si irradiated with alpha particle at a fluence of 9.3×10^{11} cm^{-2} ($f=4.6$ Hz, $V_r=2$ V, and $V_p=1.8$ V), illustrating the results of cooling with the bias-off (A state) and with applied reverse-bias (B state). The DLTS spectra derived from subtracting the two DLTS spectra (state A and B) is also shown.

indicating that some transformation did occur during the DLTS filling pulse.

No defects with concentrations above 2×10^{12} cm^{-3} could be detected by DLTS in the control (unirradiated) samples. Figure 1 shows three typical spectra after α-particle irradiation with the same fluence ($\approx9.3\times10^{11}$ cm^{-2}). The DLTS spectra that characterize the two different configurations of the defect are shown in this figure. The metastable defect (undetectable: A state) was not observed by DLTS after irradiation under normal bias conditions. The spectrum labeled state A is obtained if the specimen is cooled to the initial measurement temperature without an applied bias. The spectrum labeled state B is obtained if the specimen is cooled with a reverse-bias applied. The DLTS peak derived from the subtraction of the two DLTS spectra for the same fluence is also shown in Fig. 1. The two hole traps labeled $H\alpha1$ and $H\alpha2$ arise from two different defects. The transformation behavior of the $H\alpha2$ level is observed after zero-bias/reverse-bias cool down cycles: cooling down the sample at zero-bias causes the removal of the $H\alpha2$ signal. In contrast, cooling down at reverse-bias causes the re-introduction of defect $H\alpha2$.

In the A state, the $H\alpha1$ level has a hole emission activation energy of (0.53 ± 0.01 eV) and an apparent hole capture cross section of 1.6×10^{-13} cm^2. In the B state, peak $H\alpha$ contains contributions of $H\alpha1$ and $H\alpha2$ and has an activation energy of (0.46 ± 0.01) eV and a capture cross section of 5.3×10^{-15} cm^{-2}. An activation energy of (0.43 ± 0.01) eV and a capture cross section of 1.4×10^{-15} cm^2 were determined for $H\alpha2$. It appears that the defects labeled $H\alpha1$ and $H\alpha2$ detected in this study have the same signature as the defect detected in the same material after electron irradiation.[11]

The defect concentration profiles showed that the concentrations of $H\alpha1$ and $H\alpha2$ were very similar and constant in the region profiled (10–112 nm below the SBD interface) for each fluence investigated in this study. The introduction rates of individual defects $H\alpha1$ and $H\alpha2$ have been studied versus the fluence of α-particle irradiation in the range 1.2×10^{11}–2.2×10^{12} cm^{-2}, using the fixed-bias variable-pulse difference DLTS depth profiling in conjunction with the approach of Zohta *et al.*[12] Figure 2 shows that the concentration of $H\alpha1$ and $H\alpha2$ increases with an increase in the incident particle fluence (up to 2.2×10^{12} cm^{-3}). This suggests that these defects are either radiation-induced complexes related to impurities in the crystal of which the concentrations are higher than 2×10^{15} cm^{-3}, or a lattice defect complex independent of impurities. The DLTS signatures, the emission rates, and the introduction rates of these defects after alpha irradiation are summarized in Table I.

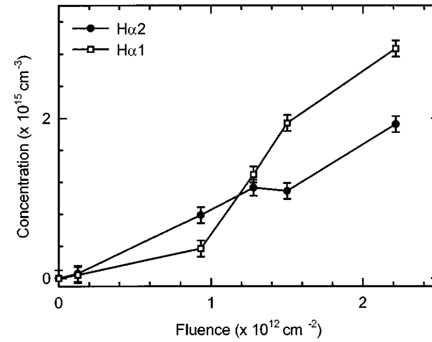

FIG. 2. Concentration of the $H\alpha1$ and $H\alpha2$ defects vs the fluence of irradiation.

We assume the metastability observed in this study is caused by the reversible transformation of the states labeled A and B. In order to examine the transition $A\rightarrow B$, the sample was first cooled from 300 K to a temperature T under zero-bias; then it was annealed for a time t at reverse-bias, and finally cooled to 130 K. The changing magnitude of $H\alpha2$ was used to determine the changing population of this A state. A similar procedure was used to study the reverse transformation $B\rightarrow A$. The results obtained after this isochronal annealing are illustrated in Fig. 3. These results show that both transformations $A\rightarrow B$ and $B\rightarrow A$ occur in a single stage, but not in the same temperature range. The first transformation ($A\rightarrow B$) takes place at a higher temperature (240–265 K) than the second transformation ($B\rightarrow A$) (185–215 K). The anneal time t was then varied at a fixed temperature T (chosen around the transition temperatures) to explore the configurational transformation kinetics. The isothermal annealing kinetics were found to be first order. Arrhenius plots for both transitions are shown in Fig. 4 (open symbols). Since a hole is emitted during the transformation from $A\rightarrow B$ (see discussion later), it was possible to observe this

TABLE I. Electronic properties and the introduction rate of the prominent hole traps, $H\alpha1$ and $H\alpha2$, introduced during alpha particle irradiation of epitaxially grown p-Si.

Defect label	Int. rate (cm^{-1})	E_t (eV)	σ_a (cm^2)	e_n[a] at 220 K (s^{-1})
$H\alpha1$	1300	0.53	1.6×10^{-13}	10
$H\alpha2$	885	0.43	1.4×10^{-15}	17
$H\alpha(H\alpha1+H\alpha2)$	⋯	0.46	5.3×10^{-15}	13

[a]Emission rate at 220 k.

University of Pretoria etd – Meyer, W E (2007)

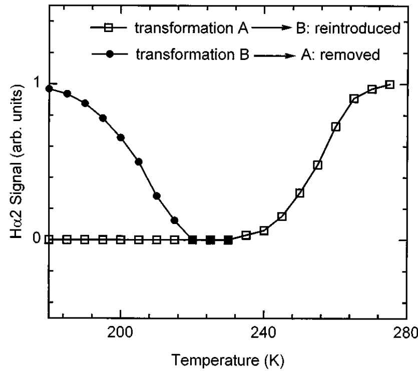

FIG. 3. Change in $H\alpha2$ peak height as a function of temperature for both transformations $A\rightarrow B$ and $B\rightarrow A$. [isochronal (5 min) annealing]. All data points have been normalized to the maximum value of this signal.

transformation directly using DLTS. Using this technique, we measured the transformation rate from state A to state B directly. By varying the filling pulse width and measuring the DLTS peak height, we could determine the transformation rate from state B to state A as well. These measurements were performed in the temperature range 260–340 K, the results of which are indicated by solid symbols in Fig. 4. The observed reaction rates can be summarized by the following relations:

$$R=(4\times10^{12}\ \mathrm{s}^{-1})\exp\left(-\frac{0.79}{kT}\right)\quad \text{for } A\rightarrow B, \tag{1}$$

$$R=(7\times10^{9}\ \mathrm{s}^{-1})\exp\left(-\frac{0.52}{kT}\right)\quad \text{for } B\rightarrow A. \tag{2}$$

The rate constant above for the transformation $A\rightarrow B$ is between that expected for carrier emission and atomic jump (10^{12}–$10^{13}\ \mathrm{s}^{-1}$), but the rate constant for the transformation $B\rightarrow A$ is slightly larger than expected for carrier capture via multiphonon emission ($R_0\approx10^{7}\ \mathrm{s}^{-1}$), but smaller than expected for carrier emission ($R_0\approx10^{12}\ \mathrm{s}^{-1}$).[13]

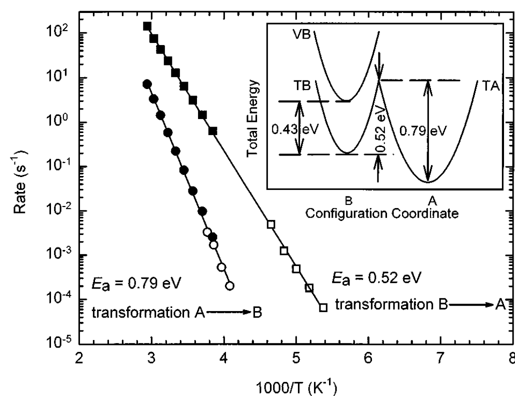

FIG. 4. Arrhenius plots of $A\rightarrow B$ and $B\rightarrow A$ transformation rates. The open and filled symbols correspond to data measured from annealing cycles and direct DLTS measurements, respectively. The configuration-coordinate (CC) diagram for the $H\alpha2$ defect is shown in the inset.

A configuration-coordinate (CC) diagram of the $H\alpha2$ defect, compatible with the above data, is shown in the inset of Fig. 4. The energy barrier for the transition from the A state to the B state is 0.79 eV and that for the reverse transformation 0.52 eV. This energy difference between the states explains the transformation temperatures as shown in Fig. 3. Because no DLTS peak associated with hole emission from state A was detected, the level associated with the empty defect in state A (VA) is not shown. However, because state B is stable under reverse bias, the total energy of the empty defect in state A should be the same or higher than that for state B. Consequently, the activation energy for hole emission from state A should be at least 0.70 eV.

In principle, there could be two different mechanisms for the transformation from state A to state B: the defect could either first emit a hole ($E_a=0.79$ eV) and then transform via a fast process, or the defect could first transform with the hole still captured ($E_a=0.79$ eV) and then emit the hole in a fast step. In both cases the rate of the transformation is determined by a step with an activation energy of 0.79 eV, and a hole is emitted during the transformation process. Since in state A the emission of a hole is either preceded or followed directly by a transformation to state B, it is not possible to observe a DLTS peak associated with state A.

In summary, we have reported the discovery of a new configurationally metastable defect, $H\alpha2$, in boron-doped epitaxially grown p-type silicon following α-particle irradiation. The results presented here indicate that $H\alpha2$ can be reversibly transformed using conventional bias-on/bias-off annealing temperature cycles. $H\alpha2$ has an energy level at (0.43 ± 0.01) eV above the valence band. The physical nature of this defect is still unknown. To this end, the correlation between results obtained from different measurement techniques and using Si with different levels of dopant and other impurities could provide useful information about the physical nature of these defects and therefore more experiments are required.

The authors gratefully acknowledge the financial assistance of the Foundation for Research Development.

[1] A. Chantre, Mater. Res. Soc. Symp. Proc. **104**, 37 (1988).
[2] C. A. Londos, Phys. Rev. B **34**, 1310 (1986).
[3] W. R. Buchwald, G. J. Gerardi, E. H. Pointdexter, N. M. Johnson, H. G. Grimmeiss, and D. J. Keeble, Phys. Rev. B **40**, 2940 (1989).
[4] M. Levinson, M. Stavola, J. L. Benton, and L. C. Kimerling, Phys. Rev. B **28**, 5848 (1983).
[5] A. Chantre and L. C. Kimerling, Appl. Phys. Lett. **48**, 1000 (1986).
[6] T. I. Kol'chenko and V. M. Lomakoi, Semiconductors **28**, 501 (1994).
[7] A. Chantre, Phys. Rev. B **32**, 3687 (1985).
[8] F. D. Auret, R. M. Erasmus, S. A. Goodman, and W. E. Meyer, Phys. Rev. B **51**, 17521 (1995).
[9] W. E. Philips and J. R. Lowney, J. Appl. Phys. **54**, 2786 (1983).
[10] D. Lang, J. Appl. Phys. **45**, 3014 (1974).
[11] M. Mamor, F. D. Auret, S. A. Goodman, W. E. Meyer, and G. Myburg (unpublished).
[12] Y. Zohta and M. O. Watanabe, J. Appl. Phys. **53**, 1809 (1982).
[13] A. Chantre, Appl. Phys. A: Solids Surf. **48**, 3 (1989).

University of Pretoria etd – Meyer, W E (2007)

PHYSICAL REVIEW B, VOLUME 63, 045201

Configurationally metastable defects in irradiated epitaxially grown boron-doped *p*-type Si

M. Mamor* and M. Willander
Physics department, Physical Electronics and Photonics, (MC2), Chalmers University of Technology and Gothenburg University, S-412 96 Gothenburg, Sweden

F. D. Auret and W. E. Meyer
Physics Department, University of Pretoria, Pretoria 0002, South Africa

E. Sveinbjörnsson
Solid State Electronics Laboratory, Department of Microelectronics ED, Chalmers University of Technology S-412 96 Gothenburg, Sweden

(Received 25 April 2000; published 22 December 2000)

In this work, we investigate the metastability of the defect $H\alpha2$ introduced in epitaxially grown boron-doped *p*-type Si by high energy (5.4 MeV) He-ion irradiation. Deep level transient spectroscopy (DLTS) and thermally stimulated capacitance (TSCAP) measurements were used to study the electronic properties of the defect in each configuration. The analyses indicate that this metastable defect can exist in either of two configurations (A or B) and can be reversibly transformed using conventional bias-on/bias-off annealing temperature cycles. The energy barriers for transition between these two configurations (A to B and B to A) are determined as 0.79 and 0.52 eV, respectively. In addition, we have compared the electronic properties of $H\alpha2$ to those introduced during high-energy (12 MeV) electron irradiation and 250 keV proton irradiation. It is shown that defect $HE2$ introduced during electron irradiation of the same epitaxially grown p-Si and a defect $HP2$ introduced during 250 keV proton-irradiated boron doped float-zone (FZ) p-Si exhibit the same metastability as $H\alpha2$ and provide further evidence that $H\alpha2$ is hydrogen-related metastable defect.

DOI: 10.1103/PhysRevB.63.045201 PACS number(s): 71.55.−i, 61.80.Jh, 61.72.Ji, 61.72.Hh

I. INTRODUCTION

Most point defects in semiconductors are observed in only one configuration. However, it is possible that a defect may exist in more than one configuration, the stable configuration or a metastable configuration depending on the charge state of the defect. The alternate (metastable) configuration of a defect can be detected experimentally through its electronic properties. Under certain experimental conditions, usually bias-on/bias-off annealing cycles, the metastable defect is configurationally transformed to different energy states which can be detected by deep level transient spectroscopy (DLTS) or thermally stimulated capacitance (TSCAP) measurements. A thorough study of configurationally bistable defects in semiconductors has been reported by Levinson.[1]

Metastable defects are important in electronic materials because the degree to which they modify semiconductors may be reversibly altered, depending on the electric field and temperature conditions. The existence of configurationally metastable defects was first revealed by electron paramagnetic resonance (EPR) studies of the oxygen-vacancy pair in Si.[2] Later DLTS and TSCAP studies have also shown the presence of an unusual metastable defect in electron-irradiated *n*-type Si as well as in *n*-type GaAs and InP.[3–5] A defect with metastable characteristics has also been observed in boron-doped float-zone (FZ) p-Si single crystals, which is tentatively identified as the substitutional boron-vacancy complex.[6,7] A defect with metastable characteristics has also been detected in aluminum-doped and boron doped silicon substrates[8,9] following ultrafast quenching (laser irradiation). Recently, a defect with metastable characteristics has also been detected in boron-doped, Czochralski-grown, Si that was electron irradiated at 80 K and is assumed to be the oxygen related metastable defect.[10] Metastable defects, however, are not limited only to the above illustrations. The DX centers in $Al_xGa_{1-x}As$ and $GaAs_xP_{1-x}$ (Ref. 11) also show metastable properties. It has been reported that alpha-particle irradiation also introduces a metastable defect in GaAs.[12] Recently, using DLTS, we observed a new metastable defect $H\alpha2$ introduced in boron-doped, epitaxially grown Si following room temperature alpha-particle irradiation.[13] This defect was found to exhibit reversible transformation between two configurations. Only in one configuration (which will be denoted as B), was the metastable defect directly observed by DLTS.

In this paper, we report the DLTS and TSCAP detection of configurationally metastable defects introduced in highly boron-doped p-Si epitaxially grown by chemical vapor deposition (CVD) following room temperature, He-ion irradiation. With new complementary investigation on this metastable defect using TSCAP, we report the observation of the metastable configuration "A." As a result, we demonstrate here evidence that the defect $H\alpha2$ can exist in either of two configurations designated A and B and exhibits two defect energy levels in the band gap. In order to investigate what kind of impurities might be involved in the configurationally metastable defect and the physical origin of this defect, we have compared the electronic properties of $H\alpha2$ to those introduced during high energy (12 MeV) electron irradiation and 250 keV proton irradiation. As a result of its electronic and metastable properties, a defect $HE2$ introduced during electron irradiation of the same epitaxially grown p-Si and a

 ©2000 The American Physical Society

University of Pretoria etd – Meyer, W E (2007)

defect $HP2$ introduced during 250 keV proton-irradiated boron doped float-zone (FZ) p-Si exhibit the same metastability as $H\alpha2$. In addition, we report on a study of the electronic properties of other defects introduced during He-ion irradiation of epitaxially grown p-Si. The He ions and electron irradiation-damage-induced defects in epitaxially grown Si are of additional interest due to the use of epitaxial materials for many devices fabrication.

In Sec. II we describe the experimental procedures involved. Section III describes the results obtained and comprises a discussion, after which some conclusions are presented in Sec. IV.

II. EXPERIMENTAL PROCEDURES

In our research we used Schottky barrier diodes (SBD's) as the diode contact structure to the boron-doped Si. Titanium SBD's on a p-type Si layer (doped to $6-8 \times 10^{16}\,\mathrm{cm}^{-3}$ with boron) grown epitaxially by chemical vapor deposition (CVD) on a p^+ Si(001) substrate, were irradiated with high energy (5.4 MeV) He ions at a fluence of $9.3\times10^{11}\,\mathrm{cm}^{-2}$, using an Americium radio-nuclide and 12 MeV electrons at a fluence of $1.6\times10^{12}\,\mathrm{cm}^{-2}$. In addition float-zone, boron-doped samples were irradiated with 12 MeV electrons and 250 keV protons to a total dose of $10^{13}\,\mathrm{cm}^{-2}$ and $7\times10^{12}\,\mathrm{cm}^{-2}$, respectively. DLTS, using a lock-in amplifier-based system, was used to study the defects. The bias and pulse sequence consisted of a reverse bias V_r on which pulses with amplitude V_p were superimposed. DLTS and TSCAP were also used to determine the electronic properties of the defects in each configuration, and the configurational transformation kinetics. The DLTS defect signatures (energy level in the band gap, E_t, and apparent capture cross section, σ_a) were calculated from the Arrhenius plots of $\ln(T^2/e)$ vs. $1/T$, where e is the emission rate at the DLTS peak temperature T. The data for the Arrhenius plots were also measured by means of an isothermal DLTS technique. Details on these experiments have been given elsewhere.[13]

III. RESULTS AND DISCUSSION

In Fig. 1 we present the DLTS spectra of Si irradiated with 5.4 MeV He ions [curves (a)]. For comparison, we also include spectra recorded from identical Si samples irradiated with 12 MeV electrons at a fluence of $1.6\times10^{12}\,\mathrm{cm}^{-2}$ [curves (b)]. The DLTS spectra for both samples were recorded under identical bias and pulse conditions: A filling pulse of amplitude $V_p = 1.8$ V was superimposed onto a quiescent reverse bias of $V_r = 2$ V. The spectra were taken after cooling the sample under zero bias (bias-off, configuration A) and after cooling with applied reverse bias (bias-on, configuration B) as shown in this figure. Curves (a) show the metastable behavior of the $H\alpha2$ defect following He-ion irradiation. The transformation behavior of the $H\alpha2$ level is observed after zero-bias/reverse-bias cool down cycles: cooling down the sample under zero-bias (configuration A: dotted line) causes the removal of the $H\alpha2$ signal. Cooling down the sample under reverse-bias causes the reintroduction of defect $H\alpha2$ (configuration B: solid line). The DLTS peak derived from the subtraction of the two DLTS spectra for the same fluence is also shown in this curve (dashed line). The two hole traps labeled $H\alpha1$ and $H\alpha2$, which are reported here, arise from two different defect levels.

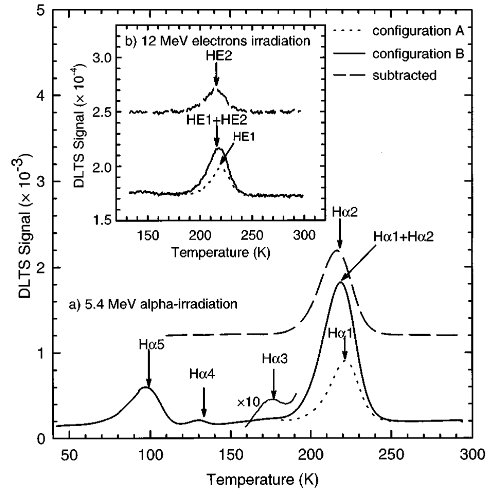

FIG. 1. DLTS spectra of p-type Si irradiated with 5.4 MeV He-ions at a fluence of $9.3\times10^{11}\,\mathrm{cm}^{-2}$, showing the result of cooling with applied zero-bias (configuration A: dotted line) and reverse-bias (configuration B: solid line). The DLTS spectrum derived from subtracting the two DLTS spectra (configuration A and B) is also shown (dashed line). The inset shows DLTS curve for 12 MeV electron irradiated p-type Si at a fluence of $1.6\times10^{12}\,\mathrm{cm}^{-2}$, showing the result of cooling with zero-bias (A) and applied reverse-bias (B).

The inset of Fig. 1 [curves (b)] shows DLTS spectra that characterize the two different configurations of the defect $HE2$ following 12 MeV electron irradiation. It appears that the defects labeled $H\alpha1$ and $H\alpha2$ have the same signature as the defects $HE1$ and $HE2$. Therefore, it is tempting to conclude that $H\alpha1$ and $H\alpha2$ are the same as $HE1$ and $HE2$, respectively.

The temperature dependence of the hole-emission rate was studied by means of an isothermal DLTS system. The results are shown in the Arrhenius plot [Fig. 2]. In configuration A, the $H\alpha1$ level has a hole emission activation energy of 0.53 ± 0.01 eV and a hole capture cross section of $(1.6\pm0.5)\times10^{-13}\,\mathrm{cm}^2$. In configuration B, peak $H\alpha$ contains contributions of both $H\alpha1$ and $H\alpha2$, and appears to have an activation energy of 0.46 ± 0.01 eV and a capture cross section of $(5.3\pm0.5)\times10^{-15}\,\mathrm{cm}^2$. An activation energy of 0.43 ± 0.01 eV and a capture cross section of $(1.4\pm0.5)\times10^{-15}\,\mathrm{cm}^2$ were determined for $H\alpha2$. An Arrhenius plot of the thermal emission rate of the defects $H\alpha3$ and $H\alpha5$ is shown in the inset of Fig. 2. The DLTS signature and peak temperature of these radiation-induced defects are summarized in Table I. The signatures of $H\alpha3$ and $H\alpha5$ were determined under low electric-field conditions (i.e., $V_r = 0.3$ V, $V_p = 0.3$ V). The activation energies of defects $H\alpha3$ and $H\alpha5$ are the same as the C_i-O_i (Ref. 14) and

University of Pretoria etd – Meyer, W E (2007)

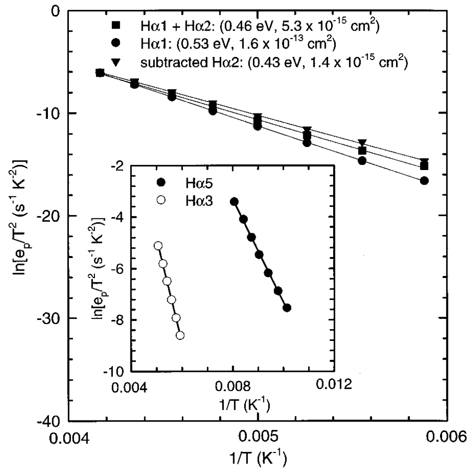

FIG. 2. Thermal emission rate data for the defect levels after cooling with bias-on (squares) and bias-off (circles). The thermal emission rate for the metastable defect is also shown (triangles). The thermal emission rates of defects $H\alpha3$ and $H\alpha5$ are shown in the inset.

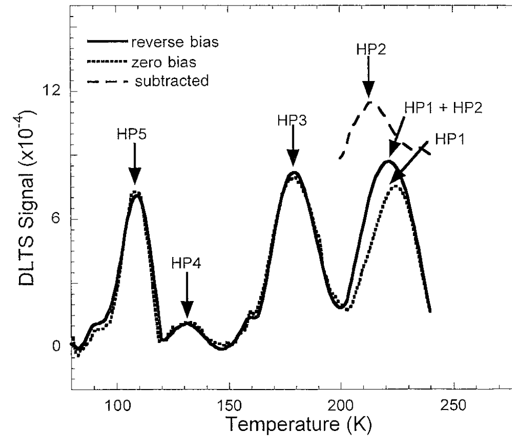

FIG. 3. DLTS spectra of a proton-irradiated, FZ, p-type silicon sample. Reverse bias$=2$ V, filling pulse$=1.8$ V and $e_p=10\,\mathrm{s}^{-1}$. The broken line shows the signature of the metastable state B obtained by subtracting the dotted spectrum (zero bias during cooling) from the solid spectrum (reverse bias during cooling).

divacancy[15] centers, respectively. A defect with a similar DLTS signature as $H\alpha1$ was detected;[16] however, the structure is as yet unresolved. The defect $H\alpha4$ was observed to anneal at room temperature after a few months with the appearance of a new defect $H^*\alpha4$ detected at $E_v+0.22\,\mathrm{eV}$.

Figure 3 shows DLTS scans of 250 keV proton-irradiated, FZ boron-doped, p-type Si and depicts the presence of the radiation-induced defects $HP1-HP5$. In this study we focus on the properties of defect $HP2$ that exhibits a metastable character. The solid line is a spectrum taken after cooling to 80 K with an applied reverse bias of 4 V applied to the sample. The temperature is then ramped up (about 5 K/min) and the spectrum is recorded. The dotted line shows a similar spectrum when the sample was cooled down to 80 K with zero bias applied to the sample. The only significant difference between the two spectra concerns the peak located at approximately 220 K, which is shifted depending on the bias during cooling. The peak has two contributions, hole emission from the state labeled B peaked at approximately 215 K (see broken line in Fig. 3) and hole emission from the state labeled A which is peaked at ≈225 K. The solid spectrum contains contributions from both states while the concentration of the B state is negligible after zero bias cooling (the dotted spectrum). The shift depends strongly upon the bias as well as the time needed to record the DLTS scan. For example if the ramp rate is reduced there is no significant difference between the two spectra and they become an intermediate between the two shown in Fig. 3. The reason for this is simply that the metastable transition takes place during the DLTS scan and a steady state between the population of the A state and the B state is reached before hole emission from the centers is recorded. The steady state ratio between the population of the states depends on the bias pulse applied during the DLTS measurement. For example, if the sample is kept at a reverse bias during the sweep and the filling pulse period is made as short as possible (10% duty cycle) the recorded spectrum is similar to the solid line in Fig. 3. If the situation is reversed and the filling pulse is on 90% of the time period, the recorded spectrum resembles the dotted line in Fig. 3. These bias-induced transformations of $HP2$ are charge state controlled and related to a reversible disappearance and reappearance of energy levels in the band gap.

TABLE I. Electronic properties of the prominent hole traps introduced during He-ion irradiation of epitaxially grown p-Si.

Defect label	E_t (eV)	σ_a (cm^2)	Peak temperature T_{peak}[a] (K)
$H\alpha1$	0.53	1.6×10^{-13}	223
$H\alpha2$	0.43	1.4×10^{-15}	215
$H\alpha(H\alpha1+H\alpha2)$	0.46	5.3×10^{-15}	220
$H\alpha3$	0.35	2.1×10^{-15}	174
$H\alpha5$	0.17	1.7×10^{-16}	102

[a]Peak temperature at a lock-in amplifier frequency of 4.6 Hz, i.e., a decay time constant of 92.3 ms.

The DLTS spectra were recorded in a somewhat unusual manner to enable detection of the metastable behavior. The transition rates, at these temperatures, from the metastable state B to state A are so high that if precautions are not taken the metastability is not observed at all.

The overall results agree very well with a study of the metastable defect $H\alpha2$ and $HE2$ in He-ion and electron-irradiated, epitaxially grown, boron-doped, p-type silicon, respectively. The hole emission rates of the metastable states are the same within experimental error and the bias dependence and transition rates between the metastable states are similar. Reference samples (FZ boron-doped p-type Si) from the same wafer without proton irradiation do not show any DLTS signatures of the metastable defect above the de-

University of Pretoria etd – Meyer, W E (2007)

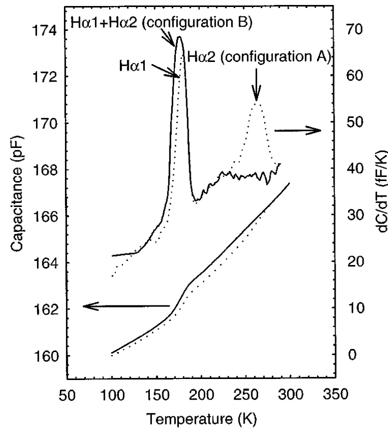

FIG. 4. TSCAP measurements of the sample shown in Fig. 1. The solid line was recorded after cooling under reverse bias while the dotted line was recorded after cooling under zero bias. In both cases the capacitance was measured at a bias of -1 V and the temperature was scanned at a rate of 3 K min^{-1}.

tection limit which is estimated to be at a concentration of 5×10^{11} cm^{-3}. The same applies to samples receiving 12 MeV electron irradiation using a fluence of 10^{13} cm^{-2}.

Concerning the differences in concentrations of the metastable defect after alpha irradiation as compared to electron and proton irradiation, we expect more damage with higher concentrations of point defects after high energy alpha irradiation as compared to low energy proton irradiation (only 250 keV) and electron irradiation. Since an alpha irradiation transfers more energy to the lattice than electron irradiation with the same kinetic energy, it is capable of forming disordered regions with a larger extent than the vacancy or interstitial defects typically observed after electron irradiation.

The remainder of this paper will concentrate on the metastability of $H\alpha2$ detected after He-ion irradiation. The metastability could also be observed by means of TSCAP measurements, as shown in Fig. 4. During these measurements, the sample was cooled under either zero or reverse bias in order to freeze in one of the metastable configurations of $H\alpha2$. After cooling to approximately 100 K, a short filling pulse was applied. Here, after a reverse bias of -1 V was applied, the temperature was increased at a constant rate of 3 K min^{-1} while the capacitance was recorded by means of an HP4192A Impedance Analyzer. Figure 4 shows the capacitance of the sample as a function of temperature, as well as its derivative dC/dT. The solid curve, which was recorded after cooling under a reverse bias of -1 V, shows hole emission from both $H\alpha1$ and $H\alpha2$ (in configuration B) at about 180 K as a rapid increase in the capacitance of the sample and a peak in the derivative curve. The dashed curve was recorded after cooling under zero bias conditions. Here the emission at 180 K is due to $H\alpha1$ only. $H\alpha2$, which has been transformed to configuration A, now emits carriers only once the temperature reaches 265 K, the same temperature at which it is transformed to configuration B. This indicates that the emission of holes from $H\alpha2$ in configuration A is closely linked to its transformation to configuration B.

The TSCAP results indicate that the transformation from configuration A to configuration B is closely associated with the emission of a hole. However, no hole emission could be observed from configuration A by means of conventional DLTS. The possible explanation for this behavior is that if the defect transforms before hole emission takes place, the hole would be emitted immediately by configuration B, because the transformation occurs at a temperature much higher than that at which configuration B starts to emit holes. This would imply that configuration A cannot be observed by means of DLTS because it transforms to state B before emitting a hole, i.e., the ionization energy of configuration A is too high for the defect to be observed by DLTS.

The transition from one configuration to the other was investigated in more detail by studying the thermally activated transformation kinetics between configurations A and B. We used the systematic method proposed by Levinson *et al.*[17,18] in their study of the metastable M center in InP. In order to examine the transition A→B, the sample was first cooled from 300 K to a temperature T at zero bias; then it was kept for a short time t at T under a fixed applied bias, and finally cooled rapidly to 130 K. The changes in the magnitude of $H\alpha2$ were used to determine the changing population of the defect in configuration A. In the same way, the reverse transition, B→A, was studied using reverse-bias cooling and zero-bias annealing. Isochronal (5 min) anneals were first performed to reveal the transformation temperature. The results obtained after this isochronal annealing (not shown here) revealed that both transitions A→B and B→A occur in only one stage, but not at the same temperature: The transformation A→B is observed at a higher temperature (240–265 K) than the transformation B→A (185–215 K). From our measurements, it seems that the transformation in both directions is complete. The reaction kinetics were then explored around the transformation temperatures by a series of isothermal anneals. The annealing reaction was found to be first order, as demonstrated in Fig. 5 for reaction A→B. Here, the normalized $H\alpha2$ peak height is plotted as a function of anneal time and temperature. The peak height of $H\alpha2$ as a function of time, $H\alpha2(t)$, was described by

$$H\alpha2(t)=H\alpha2(\infty)[1-\exp(-R_{A\to B}t)] \quad \text{A}\to\text{B}, \tag{1}$$

$$H\alpha2(t)=H\alpha2(\infty)[\exp(-R_{B\to A}t)] \quad \text{B}\to\text{A}, \tag{2}$$

where $H\alpha2(\infty)$ correspond to a peak height with $H\alpha2$ completely reintroduced.

We have also measured the transformation rate from configuration A to configuration B directly with DLTS, and from B to A by varying the filling pulse width and measuring the DLTS peak height.[13] The kinetics for the metastable defect transitions are consistent with the following relations:

$$R_{A\to B}=4\times10^{12}\exp[-(0.79\,\text{eV})/kT]\text{s}^{-1}, \tag{3}$$

$$R_{B\to A}=7\times10^{9}\exp[-(0.52\,\text{eV})/kT]\text{s}^{-1}. \tag{4}$$

Although DLTS does not provide information about the

University of Pretoria etd – Meyer, W E (2007)

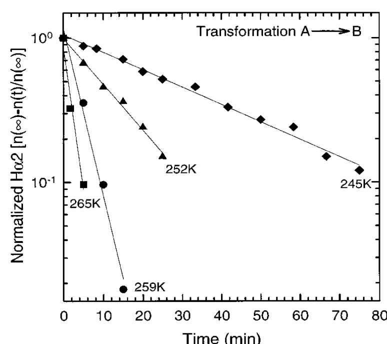

FIG. 5. Isothermal annealing kinetics for reaction A→B. For each point, the sample was cooled from 300 K to the indicated temperature with zero-bias, annealed at reverse-bias for the indicated time, and DLTS peak $H\alpha2$ was monitored.

physical nature of defects, we nevertheless have some indications as to what $H\alpha2$ may consist of. First, $H\alpha2$ and $HE2$ metastable defects have up to now been reported only in high-energy He-ion and electron-irradiated, boron-doped p-Si that was epitaxially grown by CVD and not in FZ, boron-doped, p-type Si irradiated at the same condition. Second, the same metastable defect $HP2$ is also observed in float-zone, boron-doped, p-Si following proton irradiation. In view of these facts we suggest that the metastable defect $H\alpha2$ is a hydrogen-related metastable defect due to the high concentration of hydrogen in our samples prepared by CVD and may consist of hydrogen linked to a lattice defect that was produced by the high energy bombardment.

IV. CONCLUSION

In summary, the results presented here demonstrate that one of the defects introduced in epitaxially grown, boron-doped, p-type silicon by high energy He-ion and high-energy electron irradiation, exhibits charge-state controlled metastability and can be reversibly transformed using conventional bias-on/bias-off temperature cycles. This metastable defect can exist in either of two configurations (A or B). In configuration B, $H\alpha2$ has an activation energy E_t of 0.43 ± 0.01 eV and an apparent capture cross section σ_a of $(1.4\pm0.5)\times10^{-15}\,\mathrm{cm}^2$.

The physical nature of these defects can presently at best be speculated. However, in our previous study, we have observed that the defect concentration of $H\alpha2$ increased linearly (up to $2\times10^{15}\,\mathrm{cm}^{-3}$) with increasing incident particle fluence, and no saturation effect has been seen for a fluence up to $2.2\times10^{12}\,\mathrm{cm}^{-3}$. The defect is either a radiation-induced complex related to impurities in the crystal of which the concentrations are higher than $2\times10^{15}\,\mathrm{cm}^{-3}$, or a lattice defect complex independent of impurities. Since the same metastable defect was produced by high-energy electron bombardment, it is likely to involve a lattice defect. The involvement of a lattice defect is also suggested by the nondetection of this metastable defect in similar materials irradiated with low-energy ions (<5 keV) created by the electron beam or Ar-ion bombardment. We should also notice that these metastable defects $H\alpha2$ and $HE2$ were not observed in either He-ion or electron-irradiated, FZ boron-doped p-Si, and are present only in high-energy-particle-irradiated boron-doped, p-Si, that was epitaxially grown by CVD or in proton-irradiated, FZ boron-doped, p-Si. The overall results suggest that this defect $H\alpha2$ may be either an interstitial complex, or a vacancy complexed with hydrogen.

ACKNOWLEDGMENTS

The authors thank Dr. A. Hallen, at the Royal Institute of Technology, Stockholm, Sweden for performing proton irradiation of the samples.

*Author to whom correspondence should be addressed. Present address: Institut für Physikalische Elektronik (IPE), Universität Stuttgart, Pfaffenwaldring 47, D-70569 Stuttgart, Germany; Electronic mail: Mohammed.Mamor@ipe.uni-stuttgart.de

[1] M. Levinson, J. Appl. Phys. **58**, 2628 (1985).
[2] G. D. Watkins, in *Lattice Defects and Radiation Effects in Semiconductors*, edited by F. A. Huntley (Institute of Physics, London, 1975), p. 1.
[3] O. O. Awadelkarim and B. Monemar, Phys. Rev. B **38**, 10 116 (1988).
[4] T. I. Kol'chenko and V. M. Lomakoi, Semiconductors **28**, 501 (1994).
[5] M. Stavola, M. Levinson, J. L. Benton, and L. C. Kimerling, Phys. Rev. B **30**, 832 (1984).
[6] C. A. Londos, Phys. Rev. B **34**, 1310 (1986).
[7] S. K. Bains and P. C. Banbury, J. Phys. C **18**, L109 (1985).
[8] A. Chantre and D. Bois, Phys. Rev. B **31**, 7979 (1985).
[9] A. Chantre, Phys. Rev. B **32**, 3687 (1985).
[10] C. A. Londos, Phys. Status Solidi A **133**, 429 (1992).
[11] D. V. Lang, in *Deep Centers in Semiconductors*, edited by S. T. Pantelides (Gordon and Breach, New York, 1986), Chap. 7, p. 489.
[12] F. D. Auret, R. M. Erasmus, S. A. Goodman, and W. E. Meyer, Phys. Rev. B **51**, 17 521 (1995).
[13] M. Mamor, F. D. Auret, S. A. Goodman, and W. E. Meyer, Appl. Phys. Lett. **72**, 3078 (1998).
[14] O. O. Awadelkarim, T. Gu, P. I. Mikulan, R. A. Ditizio, S. J. Fonash, K. A. Reinhardt, and Y. D. Chan, Appl. Phys. Lett. **62**, 958 (1993).
[15] B. J. Baliga and A. O. Evwaraye, J. Electrochem. Soc. **130**, 1916 (1983).
[16] P. K. Giri, S. Dhar, V. N. Kulkarni, and Y. N. Mohapatra, J. Appl. Phys. **81**, 260 (1997).
[17] J. L. Benton and M. Levinson, in *Defects in Semiconductors II*, edited by S. Mahajan and J. W. Corbett (North-Holland, New York, 1983), p. 95.
[18] M. Levinson, M. Stavola, J. L. Benton, and L. C. Kimerling, Phys. Rev. B **28**, 5848 (1983).

9

Negative-U defects in n-GaN

9.1 Introduction

A negative-U defect is a defect that can trap two electrons (or holes), with the second bound more strongly than the first. In semiconductors, negative-U ordering of defect levels leads to interesting metastability phenomena.

9.1.1 What is U?

Consider a hypothetical defect that can exist in three charge states: D^+, D^0 and D^-. I.e. if the defect is initially in the fully ionised D^+ state, it can capture two electrons. The first electron is captured according to $D^+ + e^- \rightarrow D^0$, and the second electron according to $D^0 + e^- \rightarrow D^-$. The first electron capture corresponds to a *donor* level, which is positive when it is above the Fermi level and neutral when it is below the Fermi level. Similarly, the second level corresponds to an *acceptor* level.

These two defect levels can be indicated on a band diagram as shown in Figure 9.1. Here the energy difference between the conduction band edge and the donor level is the binding energy of the first electron and the energy difference between the conduction band edge and the acceptor level is the binding energy of the second electron. Due to the Coulomb interaction between the electrons, one would expect the second electron to be more weakly bound than the first electron, and therefore the acceptor level is expected to lie above the donor level. The Coulomb interaction energy that is responsible for this phenomenon is frequently referred to as the Hubbard "correlation energy", after Hubbard (1963) who introduced it in his treatment of conductivity in narrow band semiconductors.

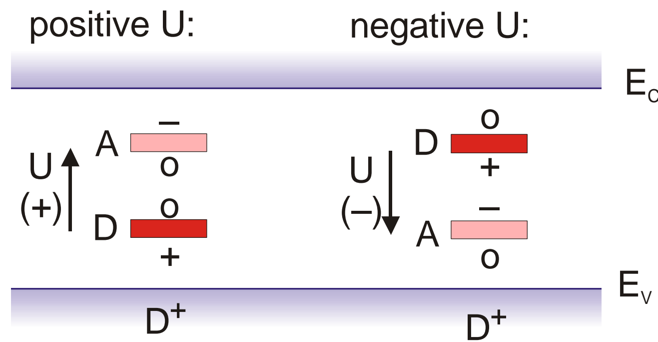

Figure 9.1 *A schematic energy-level diagram showing the behaviour of a defect D, having three charge states* D^-, D^0 *and* D^+.

Since the Coulomb interaction between two electrons is repulsive, it is quite reasonable to expect that U should always be positive. This is the case for most defects in semiconductors, however, some defects have been observed that behave as though the defect levels are inverted from their usual order, i.e. having a negative U. This implies that the second electron is *more tightly bound* than the first electron, as though there were an attractive potential between the electrons.

Negative-U behaviour is seen in a variety of physical and chemical systems ranging from disproportionation in electrochemical systems to defects in solids. An overview of a number of such systems including point defects as well as experimental evidence for these is given by Watkins (1984).

9.1.2 Mechanisms leading to negative-U behaviour

Some negative-U like properties of chalcogenide glasses were initially explained by Anderson (1975) using a model where, in addition to the restoring force the atoms exert on each other, the energy level of a state depends linearly on the displacement x between the two atoms. This model was expanded by Street (1975) and applied to point defects.

In the Anderson model, the potential energy of an atom is written in the form

$$V = -\lambda x(n_\uparrow + n_\downarrow) + \tfrac{1}{2}cx^2 , \tag{9.1}$$

where $n_\uparrow$ and $n_\downarrow$ are the occupancies (0 or 1) of the spin-up and spin-down bond orbitals. By setting $\partial V / \partial x = 0$ and substituting back in (9.1), it follows that, after relaxation, the potential energy is lowered by $-\lambda^2 / 2c$ for single occupancy and $-2\lambda^2 / c$ for double occupancy. The net effective correlation energy, defined by the energy difference between two singly occupied bonds and the disproportionated state (one empty and one doubly occupied bond) becomes

$$U_{\text{eff}} = U - \lambda^2 / c \, . \tag{9.2}$$

where U is the normal Hubbard correlation energy, that would be applicable if no lattice relaxation were present.

It follows that if λ^2/c is large enough, the correlation energy would become negative, and the disproportionated state will be energetically more favourable than two singly occupied states.

9.1.3 Properties of negative-U defects

There are a number of unusual properties that a defect with negative-U properties will have. Firstly, the neutral D^0 state is no longer thermodynamically stable. If two isolated neutral defects come into contact with each other (via the conduction band), they can lower their energy by ionizing and releasing the energy $|U|$, in a process similar to the well-known chemical phenomenon of *disproportionation* of ions in a liquid solution:

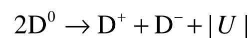

$$2D^0 \rightarrow D^+ + D^- + |U|$$

Therefore, in the ground state, a negative-U defect will always be in either the positively or the negatively ionised states, and the neutral state is always an excited state.

It follows therefore, that the donor and acceptor levels as described above, cannot be detected in the usual manner. For instance, Hall measurements would detect a single level located halfway between the donor and the acceptor levels. In the case of DLTS, if the experimental conditions are carefully chosen, it is possible to see thermal emission from both levels.

9.2 DLTS of a negative-U defect

In order to investigate how the negative-U level ordering of a defect might influence the DLTS spectrum, we first need to carefully consider how a negative-U defect behaves when the Fermi level is changed.

9.2.1 Behaviour of a negative-U defect under changing Fermi level.

The diagram in Figure 9.2 shows the energy levels of a defect D having three charge states D^-, D^0 and D^+. The energy levels shown correspond to transitions between the D^- and D^0 level (having acceptor character) and the D^0 and D^+ levels (having donor character). In the top diagram, the levels have normal (positive U) ordering, where the energy level of the donor level is below that of the acceptor, while the lower diagram shows the energy levels with negative U ordering.

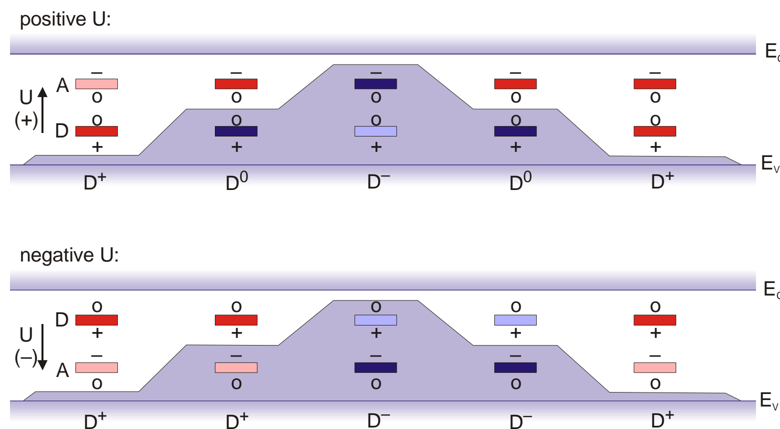

Figure 9.2 *A schematic energy-level diagram showing the behaviour of a defect D, having three charge states* D^-, D^0 *and* D^+.

Firstly consider what would happen if the Fermi level were moved from the valence band to the conduction band and back again. Initially, assume that the Fermi level is below both defect levels and that the defect is in the D^+ state (i.e. both acceptor and donor state empty), as shown at the left.

For positive U, if the Fermi level is now raised to above the donor level, it will capture an electron according to $D^+ + e^- \rightarrow D^0$. As the Fermi level is raised further, a second electron is captured when the Fermi level moves above the acceptor level, according to $D^0 + e^- \rightarrow D^-$, leaving the defect in the D^- state. If the Fermi level is now lowered again, the process is reversed, and the defect releases its first electron when the Fermi level falls below the acceptor level, and a second when the Fermi level falls below the donor level.

In the case of negative-U ordering, the matter becomes more complicated. Note that the first electron to be captured, corresponding to the donor level (i.e. $D^+ + e^- \rightarrow D^0$), has a *higher* energy than the second one. Furthermore, note that the acceptor level cannot capture an electron, because the defect is not in the D^0 state, as would be required by the reaction $D^0 + e^- \rightarrow D^-$. Therefore, as the Fermi level is raised, the defect does not capture an electron and remains in the D^+ state until the Fermi level reaches the donor level. Now the defect can capture one electron and go to its neutral D^0 state. However, as soon as the defect is in the D^0 state, the acceptor level becomes available, and since the acceptor level is also below the Fermi level, it will almost immediately capture a second electron, leaving the defect in its D^- state.

A similar situation occurs when the Fermi level is lowered. In this case, the defect does not emit an electron until the Fermi level is below the acceptor level. Once this electron is emitted, it is quickly followed by a second, since the donor level is now also above the Fermi level.

The result is that the defect with negative-U level ordering usually captures and emits two electrons in rapid succession. Furthermore, the Fermi level at which capture occurs is much higher than the Fermi level at which emission occurs. This behaviour leads to defect metastability. It is also clear that, since capture and emission of the two electrons occur in quick succession, the defect is in its unstable neutral condition for a very short time only.

9.2.2 DLTS of a negative-U defect

Figure 9.3 is a diagrammatic representation of the filling of a negative-U defect by a DLTS pulse. When a defect with negative-U level ordering is observed by means of DLTS using a relatively long filling pulse, the defect will behave in a similar fashion as we have just described – the filling pulse will fill the defect with two electrons. When the filling pulse is removed, the defect will eventually emit two electrons closely following each other. Since emission of the first electron takes much longer than emission of the second electron, the emission rate observed for this emission will essentially be that of the first electron. I.e. analysis of the DLTS signature will yield E_A .

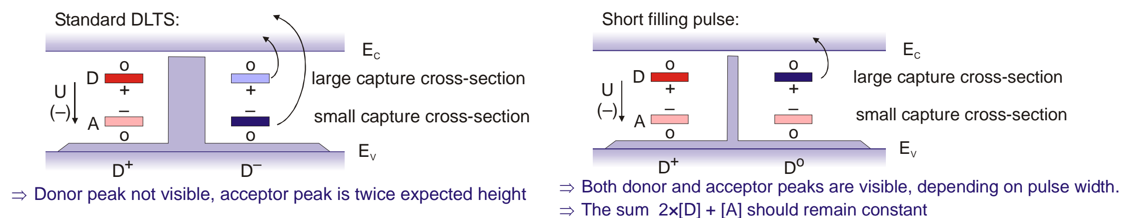

Figure 9.3 *A schematic energy-level diagram showing the behaviour of a defect D with negative U level ordering under a long and a short DLTS filling pulse.*

Since two electrons are involved, the DLTS peak will be twice as high as expected from the defect concentration. However, since the defect concentration is usually uncertain, this increase in peak height will not be noticed in a typical experimental study.

Consider, however, what would happen if a short filling pulse were applied. Since the donor level is positively charged when empty, it has a large capture cross section and will easily capture an electron. The acceptor level is neutral when empty, and will therefore have a lower capture cross-section. It follows that it might be possible, if a very short filling pulse is used, to fill mainly the donor level, leaving the acceptor level mostly empty. In this way, it could be possible to get a significant proportion of the defect in the excited D^0 state. Since the electrons in the donor state are less tightly bound than in the acceptor states, they will be emitted at a higher emission rate, as determined by E_D . Furthermore, since only a single electron was captured, only a single electron will be emitted per defect.

Thus, by varying the filling pulse length, it might be possible to vary the ratio between the number of defects that have captured only one electron, and those that have captured two electrons. In this case, the DLTS spectrum should show two peaks, one peak at high emission rates for single emission from the donor level, and a second peak with a lower emission rate, due to the emission of two electrons from the acceptor level.

As far as the peak height is concerned, the differing number of electrons per defect that are involved in each peak need to be considered. Since the acceptor level emits two electrons and the donor level only

a single electron it follows that peak heights h_A and h_D from the acceptor and donor levels respectively, should obey the relationship

$$2h_D + h_A = \text{const.} \tag{9.3}$$

The mechanism described above also leads to the paradoxical phenomenon that, after a certain filling pulse length, the height of the emission peak from the acceptor level actually *decreases* with *increasing* filling pulse length.

9.3 Negative U properties observed in a sputter-deposition induced defect in n-GaN.

The results of an investigation of sputter-deposition induced defects in OMVPE-grown n-GaN are published in the paper Auret (1999), included at the end of this chapter. In the following section, some of the aspects of this paper are discussed in more detail.

9.3.1 Introduction

Gallium nitride (GaN) is a direct, wide band gap semiconductor with a number of applications including blue and ultraviolet light emitting diodes, lasers and detectors as well as high temperature and power electronics. In the manufacturing of contacts to GaN, adhesion is a significant problem. The best adhesion results by far are obtained by sputter deposition. However, sputter deposition involves energetic particles that induce defects in the crystal lattice. In this paper, the properties of a specific defect, induced by sputter deposition of Au Schottky contacts, are discussed.

9.3.2 Experimental

The sample preparation was as described previously for GaN in Section 5.2.3. The initial measurements were performed on an LIA-DLTS system. However, after it became clear that the flexibility of the digital DLTS system was required, the measurements were continued on this system.

Since very fast pulses were required, the usual Agilent 32210 A pulse generator was used to trigger an Agilent 8110A pulse generator, which could provide much shorter pulses. Furthermore, since the internal bias filtering circuit of the Boonton 7200 would filter out such short pulses, a fast pulse interface as described in Section 4.3.1 was used to bypass the capacitance meter. By means of reed relays, the fast pulse interface could switch the sample directly to the output of the pulse generator and back in less than 1 ms, during which time the pulse was applied. During set up, care was taken to ensure that the timing of the relays was such that the sample was always connected to a reverse bias, and that there was no possibility of contact being lost due to contact bounce in the reed relays.

9.3.3 Results and discussion

Figure 9.4 shows an LIA-DLTS spectrum obtained from a sputter deposited Au Schottky contact on n-GaN. The top curve shows the DLTS spectrum of the sample, recorded after cooling the sample under a reverse bias. The second curve is of the same sample recorded under the same conditions, except that a 0.35 V forward bias was applied while the sample was at 60 K. The application of this pulse caused the ES1 peak to disappear from the spectrum that was subsequently recorded. Taking the sample to room temperature again and repeating the procedure, re-introduced the ES1 peak.

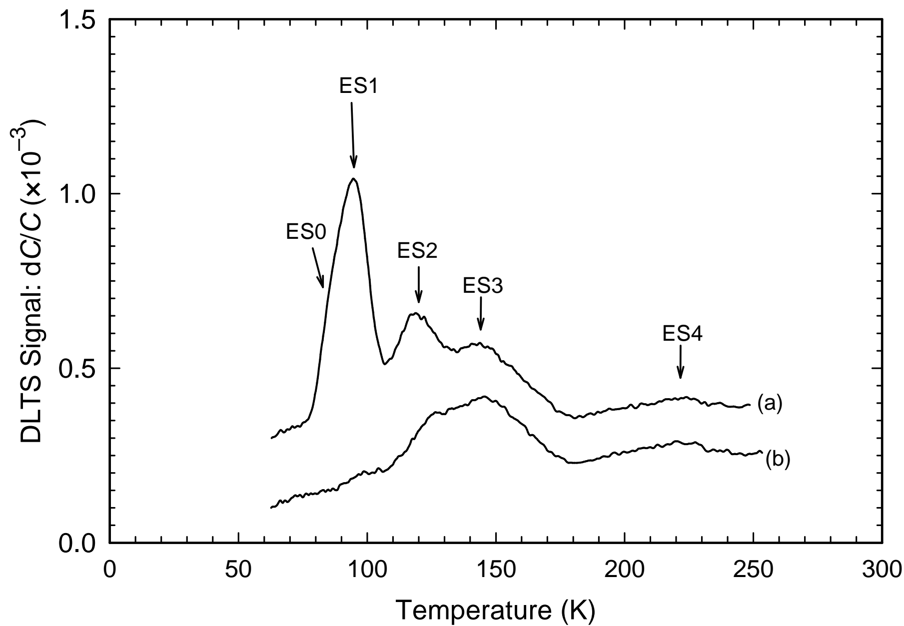

Figure 9.4 *DLTS spectra of a sputter deposited Schottky contact using* $V_r = 1.0$ V, $V_p = 1.35$ V *and* $f = 22$ Hz. *Curve (a) was recorded after cooling under reverse bias, while curve (b) was recorded after application of 0.35 V forward bias at 60 K.*

Figure 9.5 shows the isothermal DLTS spectrum obtained at 100 K, for differing pulse lengths. The spectrum shows interesting behaviour: The longer the filling pulse, the lower the amplitude of the DLTS peak. However, this is exactly the paradoxical behaviour one would expect from a negative-U defect, as discussed in section 9.2.2. As described in section 9.2.2, one possible explanation for this behaviour is that the ES1 level belongs to a defect that has another charge state in the band gap and that these levels display negative-U ordering. A short filling pulse fills only the donor level, and the associated electron is quickly released and therefore visible on the DLTS spectrum. However, when a forward bias is applied to the sample for a longer period, two electrons are captured. Since these electrons are now more tightly bound, the electrons are not emitted as fast as previously, causing the amplitude of the peak due to the donor level to decrease. As the pulse length of the filling pulse is increased, eventually all the defects will be filled with two electrons, and no transient due to the donor level will be observed.

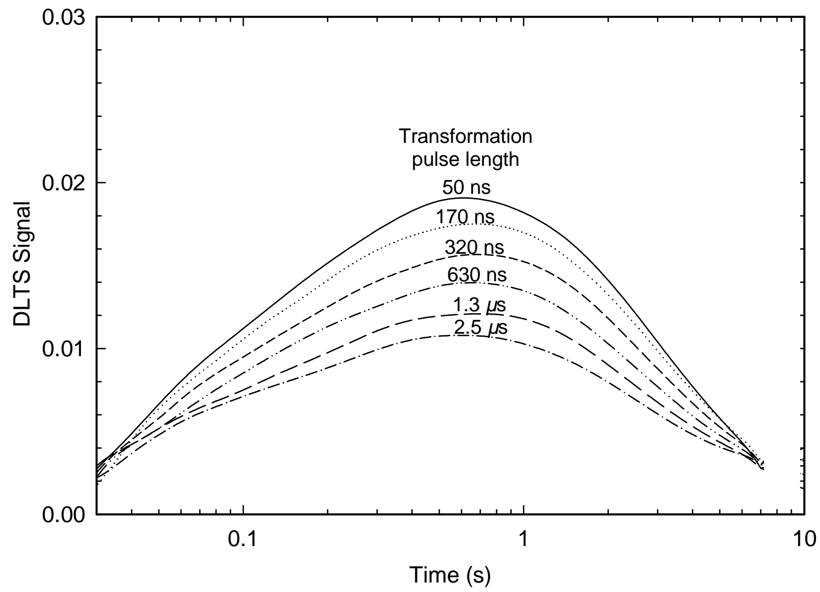

Figure 9.5 *An isothermal DLTS spectrum recorded by the digital DLTS system at 100 K (after cooling the sample from room temperature under reverse bias). The measurement conditions were* $V_r = 1.0$ V, $V_p = 1.5$ V.

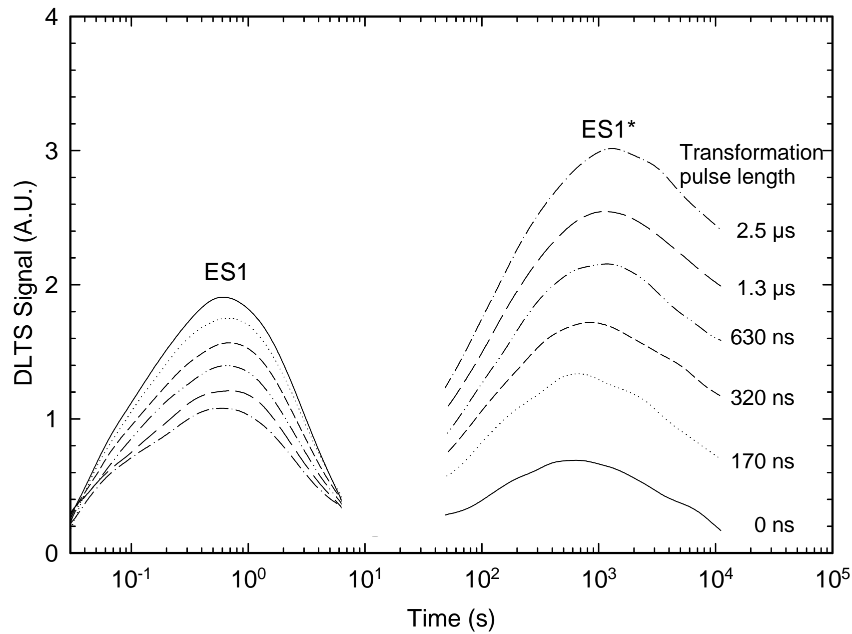

Figure 9.6 *An isothermal DLTS spectrum showing both the ES1 and the ES1* emission peaks after the application of transformation pulses of differing lengths. Recorded by the digital DLTS system at 100 K (after cooling the sample from room temperature under reverse bias). The measurement conditions were* $V_r = 1.0$ V, $V_p = 1.5$ V.

University of Pretoria etd – Meyer, W E (2007)

In this case, it seems likely that the emission rate of the peak associated with the acceptor level is so low, that it could not be detected by the LIA-DLTS system. However, since the digital DLTS system allows much longer transients to be measured, an attempt was made to detect this peak. The isothermal DLTS spectrum of the sample recorded up to 10 000 s at 100 K is shown in Figure 9.6.

The graph in Figure 9.6 shows a second peak, labelled the ES1*. The ES1* had a much lower emission rate, which explains why it could not be observed by LIA-DLTS. As expected, the height of the ES1* increased with increasing filling pulse width, and its maximum height was about twice the maximum height of the ES1.

In order to test whether the ES1 and the ES1* obey the relationship given in Equation (9.3), the DLTS transient was recorded after the application of differing lengths of transformation pulse. The exact procedure involved cooling the sample under reverse bias from room temperature to 100 K. Here after, a variable "transformation pulse" was applied. The sample was then left under reverse bias for approximately 100 seconds, after which a 50 ns filling pulse was applied and the transient recorded. The reason for this procedure was that the longer transformation pulses also filled other defects, with emission rates close to that of the ES1. By allowing the transient due to these defects to decay, and then applying a 50 ns filling pulse, the accuracy of this measurement was improved. Figure 9.7 shows the transients thus obtained.

From the transient, it is clear that there were two defect levels involved – one with a fast emission rate, and another with a slow emission rate. It can also be seen that the fast transient dominates after a short transformation pulse, while the slow transient dominates after a long transformation pulse.

The capacitance of the transient was measured 5 ms, 10s and 10 000 s after the start of the scan. The difference between the first two readings was assumed to be due to the ES1 and the difference between the second two readings was assumed to be due to the ES1*. The change in capacitance due to these two peaks for different pulse lengths is plotted in Figure 9.8.

Also plotted in Figure 9.8 is the sum of the capacitance change due to ES1 and twice the capacitance change due to ES1*. According to Equation (9.3), this should be a constant. It is interesting that, although the value remains more or less constant, there is a clear systematic sagging in the middle. It is not clear what the reason for this sagging might be.

A further prediction made by our negative-U model, is that ES1 should be a donor and ES1* should be an acceptor. As discussed in Section 2.2.3, the field dependence of the emission rate from a defect gives an indication of its charge state. The results of such a measurement are shown in Figure 9.9. Here the results were exactly as expected: Emission from the ES1 showed a significant dependence, that was well described by the three dimensional Poole-Frenkel effect, while emission from the ES1* showed very little field dependence. It is therefore reasonable to assume that the ES1 is a donor while the ES1* is an acceptor.

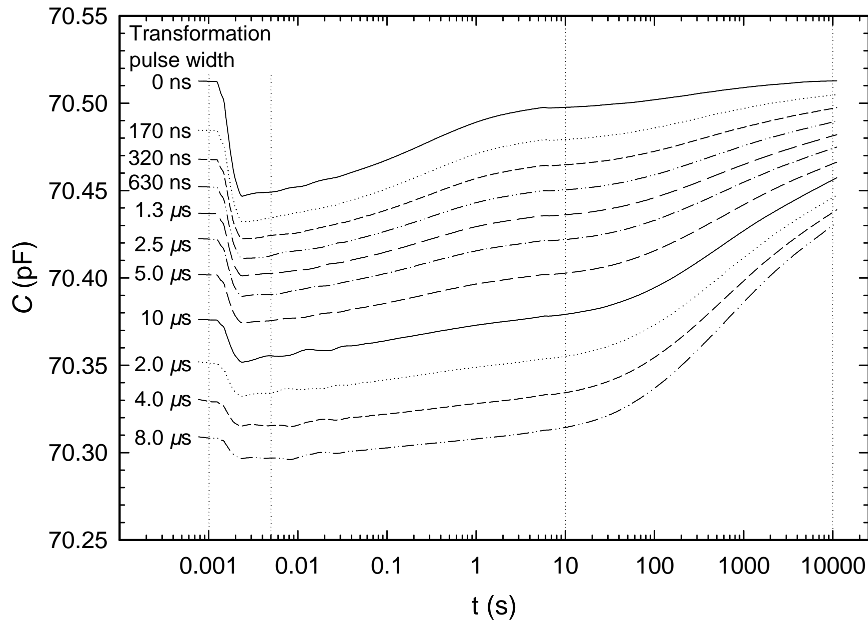

Figure 9.7 *Capacitance transients recorded from the sample after transformation pulses with differing lengths were applied to the sample. The measurements were taken at 100 K under a quiescent reverse bias of 1.0 V. The transformation pulse had an amplitude of 1.5 V and was applied 30 s before the start of the scan. The filling pulse also had an amplitude of 1.5 V, a pulse width of 50 ns, and was applied 1.5 ms after the start of the scan.*

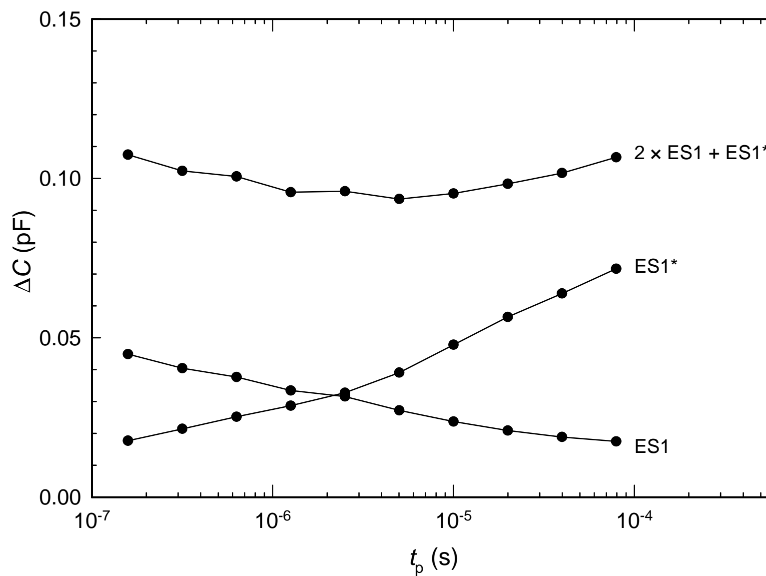

Figure 9.8 *Change in capacitance due to the ES1 and the ES1* after the application of differing transformation pulse lengths.*

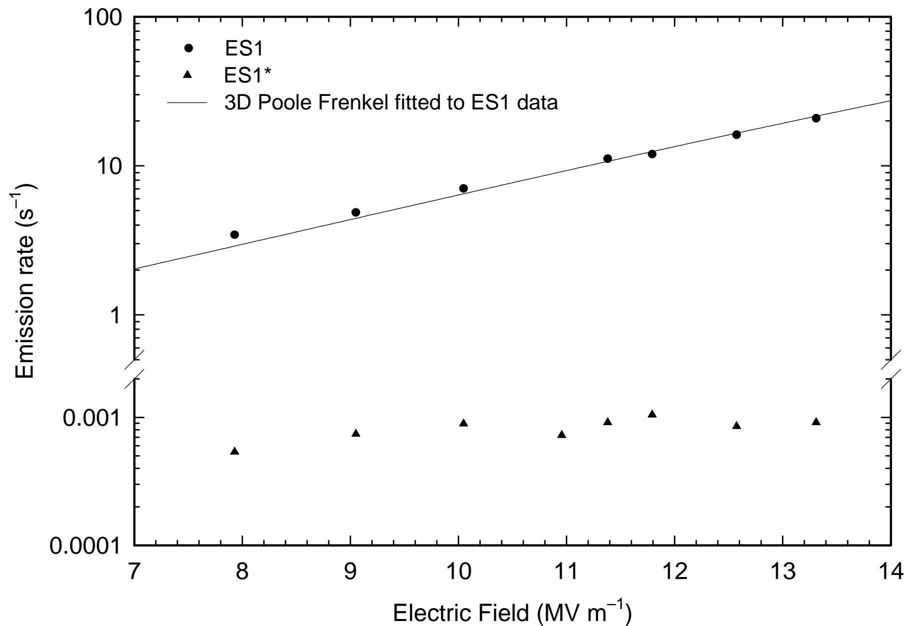

Figure 9.9 *Field dependence of the emission rate from the ES1 and ES1* level, as measured by DLTS.*

9.3.4 Conclusion

It is clear that the digital DLTS system provided a significant advantage over the analogue LIA-based DLTS system. The properties of the ES1 and ES1* levels of a sputter induced defect have been measured. ES1 and ES1* have the property that, depending on the length of the filling pulse, either ES1 or ES1* or both are visible. Over this range the quantity 2 × [ES1] + [ES1*] remains approximately constant. From the results it seems as though the ES1 and ES1* levels both belong to the same defect, that displays negative-U ordering of its energy levels. Field dependence of the emission rate from the ES1 and ES1* indicate that the ES1 is probably a donor and ES1* probably an acceptor. This is further evidence that points to negative-U properties of the defect.

9.4 Publications

The results of this investigation were published in the publication:

1. Auret FD, Meyer WE, Goodman SA, Koschnick FK, Spaeth J-M, Beaumont B and Gibart P (1999), Metastable-like behaviour of a sputter deposition induced electron trap in n-GaN *Physica B* **273-274** 92

University of Pretoria etd – Meyer, W E (2007)

ELSEVIER

Physica B 273–274 (1999) 92–95

PHYSICA B

www.elsevier.com/locate/physb

Metastable-like behaviour of a sputter deposition-induced electron trap in n-GaN

F.D. Auret[a,*], W.E. Meyer[a], S.A. Goodman[a], F.K. Koschnick[b], J.-M. Spaeth[b], B. Beaumont[c], P. Gibart[c]

[a] *Department of Physics, University of Pretoria, Pretoria 0002, South Africa*
[b] *Fachbereich Physik, Universität GH Paderborn, Paderborn, Germany*
[c] *CRHEA-CNRS, Valbonne, France*

Abstract

We show that a deep level, the ES1, introduced in n-GaN by sputter-deposition of gold Schottky contacts exhibits metastable-like behaviour during temperature cycling between 55 and 250 K. The ES1 has an energy level 0.22 ± 0.02 eV below the conduction band. We provide some evidence that indicates that the defect responsible for the ES1 has a second energy level, the ES1*, and that the metastable behaviour of the ES1 may be due to negative-U ordering of these two energy levels. Furthermore, field effect measurements indicate that the ES1 level has a donor character, while the ES1* level is probably an acceptor. © 1999 Elsevier Science B.V. All rights reserved.

Keywords: GaN; DLTS; Sputter deposition

1. Introduction

Gallium nitride, a direct, wide band-gap semiconductor, has a number of unique applications including blue, green and ultraviolet light emitting diodes, blue lasers, detectors and high temperature and power electronics devices [1,2]. An essential step in device manufacture is the deposition of a metal film that has to form ohmic or Schottky contacts to the semiconductor. This metal film is frequently deposited by means of sputter deposition. This technique has the advantage that it facilitates the stoichiometric deposition of compounds as well as the deposition of metals with a high melting point. In addition, sputter-deposited layers exhibit far better adhesion compared to layers deposited by other methods [3]. The main disadvantage of sputter deposition is that it involves energetic particles that may damage the crystal lattice and produce defects at and below the surface of the semiconductor [4]. In many cases these defects give rise to energy levels in the semiconductor band gap which are electrically active and may act as trapping or recombination levels. These defects can be observed by means of deep level transient spectroscopy (DLTS) [5].

Some defects in semiconductors exhibit charge state controlled metastable behaviour. That is, they can exist in different configurations, with the stable configuration depending on the charge state of the defect [6]. Such charge state controlled metastability allows for the reversible introduction and removal of defects in a semiconductor, and leads to a number of interesting phenomena, for instance the number and energy of the deep levels observed in a sample may depend on the bias conditions under which the sample was cooled. The metastability of defects is also of technologically importance, since the presence of a metastable defect in a device may lead to electrical properties that depend on the history of the sample, thus leading to unreliable device characteristics.

In this paper we discuss some of the metastable properties of defects introduced in n-GaN during sputter deposition of Au Schottky contacts.

* Corresponding author. Tel.: + 27-12-420-2684; fax: + 27-12-362-5288.

E-mail address: fauret@scientia.up.ac.za (F.D. Auret)

0921-4526/99/$ - see front matter © 1999 Elsevier Science B.V. All rights reserved.
PII: S0921-4526(99)00414-7

University of Pretoria etd – Meyer, W E (2007)

2. Experimental procedure

We used epitaxial n-GaN grown by organo-metallic vapour-phase epitaxy (OMVPE), with a free carrier density of $2–3 \times 10^{16}\ \mathrm{cm}^{-3}$ as determined by capacitance–voltage (CV) measurements. The samples were cleaned [7] by boiling them in aqua-regia. After rinsing the samples in de-ionized water, the samples were degreased in boiling trichloroethylene followed by rinsing in boiling isopropanol and in de-ionized water. Finally, the samples were dipped in a 50% HCl solution for 10 s. Ohmic contacts, consisting of 150 Å/2 200 Å/400 Å/500 Å layers of Ti/Al/Ni/Au [8], were deposited by means of electron beam evaporation and annealed at 500°C for 5 min in Ar. The samples were again degreased and dipped in a 50% HCl solution before deposition of the Schottky contacts. The Schottky contacts, 0.5 mm in diameter and 1 μm thick were sputter-deposited on the GaN through a metal contact mask [9]. For control purposes, Au SBDs were resistively deposited next to the sputter deposited SBDs.

The defects were characterized by means of a lock-in amplifier (LIA) based DLTS system, using a Boonton 7200 capacitance meter and a Stanford Research model SR830 LIA, which facilitates transient analysis at pulse frequencies as low as a few mHz. In order to measure single-shot events, an isothermal DLTS system was used. In this system, the capacitance transient from the Boonton 7200 was captured by an HP 3458 A multimeter and processed by a microcomputer. This isothermal DLTS system also allowed the measurement of DLTS transients lasting as long as a couple of hours. Therefore, it was possible to observe defects at temperatures much lower than those at which they are commonly observed by an LIA-based DLTS system.

The energy level in the band gap, E_T, and the apparent capture cross section σ_n of the defect (collectively known as the defect's 'signature'), were calculated from Arrhenius plots of T^2/e versus $1/T$, where e is the emission rate at temperature T.

In order to allow for measurements with short (down to 50 ns) filling pulses, a set of reed relays were used to connect the sample directly to the pulse generator and to disconnect the capacitance meter from the sample. To ensure that the sample was not inadvertently exposed to a filling pulse care was taken to ensure that the capacitance meter was only disconnected after the pulse generator was connected to the sample and no more contact-bounce was observed. Special precautions were taken to avoid any pulses being applied to the sample prior to the measurements. The absence of filling pulses was confirmed by monitoring the voltage across the samples with a fast (200 MHz) storage oscilloscope.

3. Results and discussion

The DLTS spectra of the resistively deposited control sample as well as the sputter-deposited diodes are shown in Fig. 1 curves (a) and (b), respectively. The energy levels and apparent capture cross sections of the sputter-induced defects are summarized in Table 1 [10].

Fig. 2 illustrates the metastable properties exhibited by the ES1 defect. Both curves (a) and (b) were recorded after cooling the sample under reverse bias. However, before curve (a) was recorded, the sample was exposed to a forward bias of 0.35 V. This forward bias pulse seems to reversibly remove the ES1 and ES2 defects. Both defects could be re-introduced by heating the sample under reverse bias to over 150 K. Further investigation using the isothermal DLTS system, showed that the height of the ES1 defect was decreased by an increase in the length of the filling pulse. This is contrary to the usual case, where an increase in the length of the filling pulse increases the height of the DLTS peak. It seems therefore that the capture of an electron in some way decreases the height of the ES1.

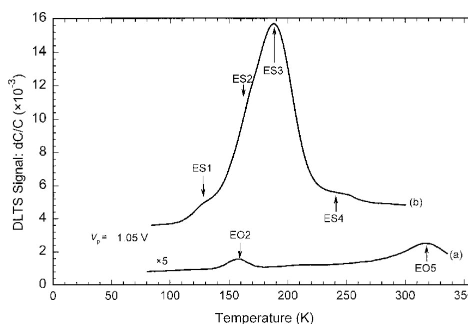

Fig. 1. DLTS spectrum of a resistively deposited control SBD (curve (a)) and a sputter deposited Schottky barrier (curve (b)) on epitaxial GaN ($V_p = 1.2$ V, $t_p = 0.2$ ms, $f = 46$ Hz).

Table 1
Electronic properties of sputter deposition induced defects in epitaxial n-GaN

Defect label	E_T (eV)	σ_a (cm^2)	T_{peak}[a] (K)
ES0	—	—	—
ES1	0.22 ± 0.02	$6.5 \pm 2.0 \times 10^{-16}$	< 120
ES2	0.30 ± 0.01	$4.4 \pm 1.0 \times 10^{-14}$	157
ES3	0.40 ± 0.01	$3.3 \pm 1.0 \times 10^{-13}$	192
ES4	0.45 ± 0.10	$8.1 \pm 2.0 \times 10^{-16}$	249

[a] Peak temperature at a lock-in amplifier frequency of 46 Hz, i.e. a decay time constant of 9.23 ms.

University of Pretoria etd – Meyer, W E (2007)

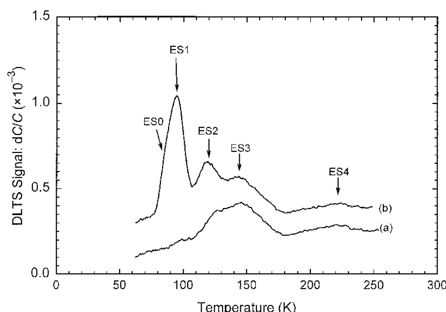

Fig. 2. DLTS spectra of a sputter deposited Schottky contact using $V_r = 1.0$ V, $V_p = 1.35$ V, $f = 0.22$ Hz. Curve (a) was recorded after cooling under reverse bias, while curve (b) was recorded after application of 0.35 V forward bias at 60 K.

One possible explanation for this behaviour is a phenomenon known as negative-U [11]. According to this explanation, the ES1 defect is one energy level of a defect that has two energy levels in the band gap (i.e. the defect can trap two electrons). If the defect has already captured one electron, the second electron the defect captures would be repelled by coulomb interactions with the first electron. This implies that the second electron should be less tightly bound than the first electron. This difference in binding energy is referred to as U, and is usually positive. However, in some defects, there may be some interaction with the lattice that causes the second electron to be more tightly bound than the first, i.e. U is negative. A classical case in which negative-U properties have been demonstrated is the boron interstitial in silicon [12].

In the case of the ES1 deep level, the short (50 ns) filling pulse is just long enough to fill the defect with one electron. After the defect has captured one electron, the capture cross section of the defect decreases dramatically, due to the change in the charge state of the defect. Therefore, the defect will not capture another electron as easily as it captured the first. After the filling pulse, the electron is easily emitted and gives rise to the ES1 peak observed in the DLTS spectrum.

If a long filling pulse is applied, the defect will capture a second electron. However, due to the negative-U ordering of these two energy levels, the second electron to be captured is more tightly bound than the first. Therefore this electron is emitted at a significantly lower rate than the first, and should give rise to another defect level with a lower emission rate, which we shall refer to as the ES1*. The first electron to be emitted is now rapidly followed by the emission of a second electron to be emitted (since the second electron is more weakly bound than the first). This implies that the ES1* should have twice the height of the ES1.

If a filling pulse with a length falling between the two extremes is applied, some of the defects will have captured a single electron, while others will have captured two electrons. Emission from these defects will give rise to both the ES1 and the ES1* DLTS peaks. It follows from the above argument that the heights of the peaks should be related by

$$2 \times [\text{ES1}] + [\text{ES1*}] = \text{constant}. \quad (1)$$

In order to investigate the possibility of the ES1 belonging to a defect having negative-U properties, an attempt was made to look for evidence of a second energy level. Further investigations with the isothermal DLTS system showed that, as the peak due to the ES1 disappeared, a second peak with a much lower emission rate appeared. This second peak will be referred to as the ES1*. The isothermal DLTS spectrum obtained for the ES1 and ES1* after the application of different filling pulses is shown in Fig. 3. Here it can be clearly seen that the height of the ES1* (peak at 1000 s) increases as the height of the ES1 (peak at 0.6 s) decreases.

In order to confirm the relationship predicted by Eq. (1), the charge involved in each of the DLTS peaks was estimated by measuring the change in capacitance associated with each of the peaks. Fig. 4 shows this capacitance change for both peaks as a function of filling pulse length. Also shown is the value of $2 \times [\text{ES1}] + [\text{ES1*}]$, which is approximately constant. The systematic deviation observed should still be investigated further, but it could be due to the field dependence of the emission rate or an inaccurate determining of the baseline position of partly overlapping peaks in Fig. 3.

In order to obtain some further insight into the properties of the ES1 and the ES1*, the field dependence of the emission rate from these defects was determined. This property is frequently used to estimate the shape of the potential well of a defect and to distinguish between

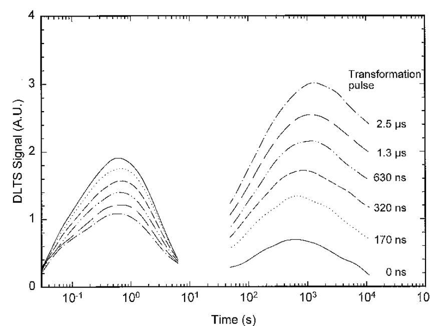

Fig. 3. Isothermal DLTS spectra obtained after the application of filling pulses with different lengths. Note that the height of the ES1 peak (at 0.6 s) decreases as that of the ES1′ (at 1000 s) increases. ($V_r = -1$ V, $V_p = 1.5$ V, $T = 100$ K).

University of Pretoria etd – Meyer, W E (2007)

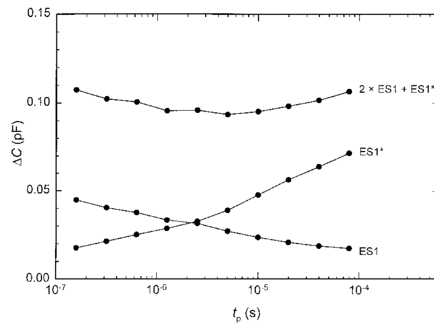

Fig. 4. Capacitance change associated with the ES1 and the ES1* after the application of different filling pules. The third curve corresponds to $2\times[\mathrm{ES1}]+[\mathrm{ES1}^*]$.

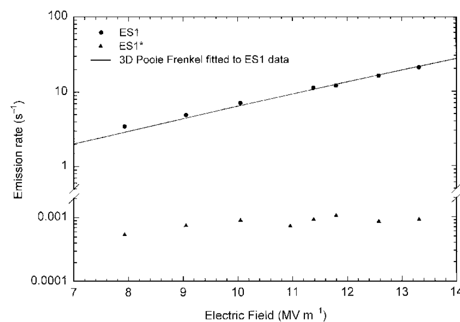

Fig. 5. Field dependence of the emission rate from the ES1 and ES1* defects as determined by means of isothermal DLTS at 100 K.

donor and acceptor levels [13]. The results of these measurements are shown in Fig. 5, which shows that the emission from the ES1 is strongly field dependent while the emission from the ES1* is much less dependent on the electric field.

If it is assumed that the field enhanced emission from the ES1 and ES1* is due to the Poole–Frenkel lowering of the barrier height, it follows that the potential well of the ES1 has to be much wider than that of the ES1*. A more quantitative approach can be followed by fitting the theoretical curve for the Poole–Frenkel field enhanced emission from a Coulombic well [13] to the field dependent emission data obtained for the ES1 (see Fig. 5). The excellent fit obtained indicates that the field enhanced emission from the ES1 is consistent with the Poole–Frenkel emission from a three-dimensional coulombic well, and therefore the ES1 is probably a donor. The weak dependence of the emission from the ES1* on the electric field, combined with the lower capture cross section, indicates that the ES1* is probably an acceptor.

4. Conclusions

We have reported some of the transformational properties of a sputter-induced metastable defect in n-GaN. The unusual transformational properties of the defect can be explained by assuming that the defect has two energy levels in the band gap, ES1 and ES1*, with negative-U ordering. The ES1 level is the same level that was previously reported in n-GaN with an energy level 0.22 ± 0.02 eV below the conduction band. We have used field effect measurements to show that this level is probably a donor. In contrast to the ES1, emission from the ES1* is much less sensitive to the electric field. It is therefore speculated that the ES1* is an acceptor. Although the evidence for the negative-U properties of this defect is not conclusive, it is hoped that further investigation could provide a definite answer.

Acknowledgements

We gratefully acknowledge financial assistance from the South African Foundation for Research Development. We also thank G. Myburg for ohmic contact metallization and C. Schutte and C. du Toit for sputter deposition.

References

[1] S. Nakamura, G. Fasol, The Blue Laser Diode, Springer, Berlin, 1997.
[2] K. Doverspike, A.E. Wickenden, S.C. Binarii, D.K. Gaskill, J.A. Freitas, Mater. Res. Soc. Symp. Proc. 395 (1996) 897.
[3] L.I. Maissel, in: L.I. Maissel, R. Glan (Eds.), Handbook of Thin Film Technology, McGraw-Hill, New York, 1970, pp. 1–4.
[4] F.H. Mullins, A. Brunnschweiler, Solid State Electron. 19 (1976) 47.
[5] D.V. Lang, J. Appl. Phys. 45 (1974) 3023.
[6] A. Chantre, Appl. Phys. A 48 (1989) 3.
[7] P. Hacke, T. Detchprohm, K. Hiramatsu, N. Sawaki, Appl. Phys. Lett. 63 (1993) 2676.
[8] S. Ruvimov, Z. Liliental-Weber, J. Washburn, K.J. Duxstad, E.E. Haller, Z.-F. Fan, S.N. Mohammed, W. Kim, A.E. Botchkarev, H. Morkoc, Appl. Phys. Lett. 69 (1996) 1556.
[9] F.D. Auret, S.A. Goodman, F.K. Koschnick, J.-M. Spaeth, B. Beaumont, P. Gibart, Appl. Phys. Lett. 74 (1999) 2173.
[10] F.D. Auret, S.A. Goodman, F.K. Koschnick, J.-M. Spaeth, B. Beaumont, P. Gibart, Mater. Sci. Eng. (1999), submitted for publication.
[11] G.D. Watkins, Negative-U properties for Defects in Solids, Festkörperprobleme XXIV, 1984, p. 163.
[12] J.R. Troxell, G.D. Watkins, Phys. Rev. B 22 (1980) 593.
[13] J.L. Hartke, J. Appl. Phys. 39 (1968) 4871.

University of Pretoria etd – Meyer, W E (2007)

10 Conclusions

The research contained in this thesis is an excerpt of the investigations done by means of the digital DLTS system. Conclusions specific to each of the experimental sections are given in the text or in the included papers. In this section, the conclusions regarding the digital DLTS system are summarised.

Selection and characterisation of the instrumentation

The study showed that it is important that great care be taken in selecting the instrumentation for the DLTS system. Rough guidelines regarding the specifications of the equipment are given in Chapter 4.

A number of pulse generators were investigated and it was found that some of the less expensive pulse generators, such as the Agilent 33120A performed much better than more expensive models. Also, a number of modifications and additions to the standard DLTS set up, that allowed special measurements to be made, were described.

Characterisation of the EL2 and the E2 defect in n-GaAs

The emission from the EL2 defect in n-GaAs could be measured over a much wider temperature range than would be possible with an analogue DLTS system. The results obtained for the EL2 agree well with results previously obtained by means of an analogue DLTS system, as well as with the values quoted in literature. The results indicate that the digital system could accurately measure emission rates from below 10^{-3} s^{-1} to more than 10^{3} s^{-1}.

The ability of the digital DLTS system to measure very long transients allowed the observation of unusual phenomena, such as emission from the E2 defect stimulated by thermal radiation from the inner shroud of the cryostat.

Field dependence of the thermally activated emission rate

The field-enhanced emission from a number of defects was measured. The results appear in the relevant papers referenced in Chapter 7. The results agreed well with the relevant theory.

DLTS observation of the transformation of bistable defects

The digital DLTS system allowed single transients to be digitised. This made it possible to characterise the transformation of a metastable defect in *p*-Si much more accurately than was possible with an analogue system. This research clearly shows the superiority of the digital system when compared to an analogue system.

Negative-U defects in n-GaN

Again, the ability of the digital DLTS system to analyse single transients allowed the properties of a sputter-deposition-induced defect in *n*-GaN to be analysed in detail. The results obtained give strong evidence that the defect has negative-U properties. As was the case with the previous investigation, it would certainly not be possible to obtain these results using an analogue DLTS system.

General

It is clear that the digital DLTS system described in this thesis has a number of advantages over the analogue LIA-based system. These include:

- A wider range of emission rates (both longer and shorter) could be observed;
- The isothermal technique allows for more accurate temperature determination;
- "Single shot" measurements allowed the observation of phenomena that are not observable in a LIA-based system;
- Wide variations in pulse length can easily be accommodated;
- Digital acquisition of the capacitance transient allows for measurements on a single transient.

Further research

Since the original design and construction of the system, there were huge advances in the computational power and ADC technology. A more modern system, controlled by a friendlier user interface such as LabView, using a commercial ADC card, might give even more flexibility at lower cost. Furthermore, computational power is now fast enough to allow for more advanced analysis techniques, for instance the Gaver-Stehfest analysis technique investigated by Istratov.